JOURNAL OF BONE AND MINERAL RESEARCH
Volume 19, Number 2, 2004
Published online on December 16, 2003; doi: 10.1359/JBMR.0301229

Estrogen Regulates the Production of VEGF for Osteoclast Formation and Activity in *op/op* Mice

Ichiro Kodama,[1,2] Shumpei Niida,[2,3] Mitsuhiro Sanada,[1] Yuji Yoshiko,[2] Mikio Tsuda,[1] Norihiko Maeda,[2] and Koso Ohama[1]

ABSTRACT: *op/op* mice have a severe deficiency of osteoclasts because of lacking functional M-CSF that is an essential factor of osteoclast differentiation and function. We now report that OVX induces osteoclast formation and cures osteopetrosis by increasing the VEGF that regulates osteoclast formation in these mice.

Introduction: We have found that estrogen deficiency induced by ovariectomy (OVX) upregulated osteoclast formation in *op/op* mice. We have recently demonstrated that vascular endothelial growth factor (VEGF) could substitute for macrophage colony-stimulating factor (M-CSF) in the support of osteoclastic bone resorption in these mice. Therefore, in this study, we wished to assess the effects of VEGF on bone loss induced by OVX in these mice.
Materials and Methods: Eight-week-old *op/op* mice were bilateral OVX or sham-operated. Mice were killed at 8, 10, and 12 weeks of age, and femurs were removed for preparations. Some OVX mice were treated with three consecutive injections of 120 μl/body of VEGF-neutralizing antibody at 12-h intervals starting from 36 h before death at 4 weeks after OVX. VEGFR-1/Fc chimeric protein (600 μg/kg/day) or 17β-estradiol (0.16 μg/day) was administered in a dorsal subcutaneous pocket of the mice at the time of OVX. These mice were killed 2 weeks after surgery. Changes of serum levels of VEGF were measured by ELISA. Changes of mRNA levels of VEGF, Flt-1, interleukin-6, and osteoclast differentiation factor (ODF/TRANCE/RANKL) in bone tissue were measured by reverse transcriptase-polymerase chain reaction.
Results: In OVX *op/op* mice, trabecular bone volume of the femur was decreased, and the number of osteoclasts was significantly increased. Serum levels of VEGF were demonstrated to be higher in OVX mice than in sham-operated mice. VEGF mRNA, Flt-1 mRNA, interleukin-6 mRNA, and RANKL mRNA levels in bone tissue were elevated in OVX mice over that in sham-operated mice. The increase in osteoclast number was inhibited by VEGF antagonist treatment in OVX mice.
Conclusions: In this study, we have demonstrated that the production of VEGF and RANKL stimulated by OVX results in increased osteoclast formation in *op/op* mice.
J Bone Miner Res 2004;19:200–206. Published online on December 16, 2003; doi: 10.1359/JBMR.0301229

Key words: estrogen, vascular endothelial growth factor, osteopetrosis, osteoclast, bone resorption

INTRODUCTION

IT IS RECOGNIZED THAT one of the mechanisms by which estrogen deficiency[1] causes bone loss is through stimulating the generation of osteoclasts. Macrophage colony-stimulating factor (M-CSF) is essential for the proliferation and differentiation of osteoclast precursors.[2] Additionally, treatment of cultured bone marrow cells with anti–M-CSF antibodies blocked the formation of osteoclasts. These data suggest that M-CSF plays a critical role in murine osteoclastogenesis. Stromal cell production of M-CSF is induced by interleukin-1 (IL-1) and TNF-α and TNF-β,[3] cytokines produced mainly by bone marrow mononuclear cells[4] and recognized for their ability to promote osteoclast formation and bone resorption.[5,6] A soluble form of RANKL (also known as OPGL, TRANCE, or ODF) can promote osteoclast formation in the absence of stromal cells, but this activity depends on the additional presence of M-CSF.[7,8]

op/op mice homozygous for the recessive mutation, osteopetrosis (*op*), on chromosome 3 have a severe deficiency of osteoclasts, monocytes, and macrophages in various organs.[9,10] However, severe osteopetrosis in *op/op* mice is evident only during their youth and is progressively corrected in association with an increase of osteoclasts.[11] Previously, we demonstrated that the angiogenic cytokine vascular endothelial growth factor (VEGF) could substitute for M-CSF in osteoclast recruitment in *op/op* mice lacking functional M-CSF.[12] Furthermore, we found that estrogen deficiency caused by ovariectomy (OVX) led to an increase in osteoclastic bone resorption in *op/op* mice. In this study,

The authors have no conflict of interest.

[1]Department of Obstetrics and Gynecology, Graduate School of Biomedical Sciences, Hiroshima University, Hiroshima, Japan; [2]Department of Oral Growth and Developmental Biology, Graduate School of Biomedical Sciences, Hiroshima University, Hiroshima, Japan; [3]Department of Geriatric Research, National Institute for Longevity Sciences (NILS), Aichi, Japan.

we assessed the effects of VEGF on the bone loss caused by OVX-induced estrogen deficiency in *op/op* mice.

MATERIALS AND METHODS

Mice and monoclonal antibodies

op/op mice and their normal littermates (NLMs; +/?) were raised in our animal facility as described previously.[13,14] Mice of *op/op* genotype were identified at the 11th day of age by the absence of incisor eruption. Eight-week-old *op/op* mice were subjected to either dorsal OVX or sham operation under general anesthesia. Some OVX mice were treated with VEGF neutralizing antibody (R&D Systems, Minneapolis, MN, USA), recombinant human Flt-1/ Fc chimera (R&D Systems), or 17β-estradiol as indicated. VEGF neutralizing antibody and recombinant human Flt-1/Fc chimera bind VEGF and placenta growth factor (PlGF) with high affinity and are potent VEGF antagonists. Flt-1/ Fc chimera (600 μg/kg/day) was administered by implanting Alzet 1002 osmotic pumps (Alza Inc., Palo Alto, CA, USA) in a dorsal subcutaneous pocket at the time of surgery (VEGF antagonistic study 1). 17β-estradiol (0.16 μg/day, the lowest dose that maintains a normal uterine weight) was administered using slow-release subcutaneous pellets (Innovative Research of America, Toledo, OH, USA) in a dorsal subcutaneous pocket at the time of surgery. Flt-1/Fc chimera–injected mice and 17β-estradiol–administered mice were killed 2 weeks after surgery. VEGF neutralizing antibody (120 μl/body) was injected subcutaneously every 12, 24, and 36 h before death. VEGF neutralizing antibody–injected mice were killed at 4 weeks after surgery (VEGF antagonistic treatment study 2). Two, 4, 6, 8, and 10 weeks after surgery, mice were killed to obtain blood and bone tissues.

Histological observations

op/op mice were anesthetized with ether and perfused with 4% periodate-lysine-paraformaldehyde fixative solution (pH 7.4) through the descending aorta. Femurs were decalcified in 10% EDTA (pH 7.0) for 28 days and embedded in paraffin. Longitudinal sections (7 μm thick) of the median portion of whole femurs were stained for TRACP activity as described previously[13,15] and counterstained with methyl green. $TRACP^+$ cells with two or more nuclei were counted as osteoclasts. Some sections were stained by Mallory's azan staining.

Measurement of serum VEGF, IL-1α, and TNF-α concentration by ELISA

Serum was separated by centrifugation at 800*g* for 10 minutes at 4°C. The samples were stored at −80°C until assayed.

VEGF and TNF-α assays were performed using a Sandwich Enzyme Immunoassay kit for mouse VEGF and mouse TNF-α (Quantikine; R&D Systems) according to the manufacturer's instructions. IL-1α was assayed using a Sandwich Enzyme Immunoassay kit for mouse IL-1α (ENDOGEN, Inc., Woburn, MA, USA) according to the manufacturer's instructions.

Preparation of total RNA and reverse transcriptase-polymerase chain reaction analysis

Powdered frozen bone tissue was lysed by the addition of 1 ml Trizol reagent (Life Technologies, Gaithersburg, MD, USA), and total RNA was prepared per the manufacturer's instructions.

Single-stranded cDNA was synthesized from 1 μg of total RNA in the presence of Rever Tra Ace (TOYOBO) and the oligo (dT) primers according to the manufacturer's instructions.

cDNA was amplified by polymerase chain reaction (PCR) to generate products corresponding to mRNA encoding the gene products listed as follows: VEGF forward, 5′-CAAGGCTCACAGTGATTTTCTGGC-3′; VEGF reverse, 5′-GAAGTCCCATGAAGTGATCAAG-3′[16]; Flt-1 forward, 5′- GTACAACACCACGGAGTTGTA-3′; Flt-1 reverse, 5′-TCACCTGGACTGAGACCAAG-3′[17]; IL-1α forward, 5′-GCTCACGAACAGTTGTGAATCTG-3′; IL-1α reverse, 5′-CAGGATGTGGACAAACAC-3′[18]; TNF-α forward, 5′-ACATTCGAGGCTCCAGTGAATTCGG-3′; TNF-α reverse, 5′-GGCAGGTCTACTTTGGAGTCATTGC-3′[19]; IL-6 forward, 5′-GCTTCTGTGACTCCAGCTTATCT-3′; IL-6 reverse, 5′-ATGAAGTTCCTCTCTGCAAGAG-3′; RANKL forward, 5′-AGCTGAAGATAGCTCTGTAGG-TACGC-3′; RANKL reverse, 5′-CAGCACTCACTGC-TTTTATAGAATCC-3′.[20] The 50-μl amplification mixture contained 0.5 μg of template cDNA, 0.25 μl of *Taq*DNA polymerase (QUIAGEN GmbH, Hilden, Germany), 2.5 pmol each of the 5′ and 3′ primers, 10 mM dNTPs (GIBCO BRL, Gaithersburg, MD, USA), 5 μl of 10× reaction buffer, 10 μl of 5× Q buffer, and sterile H_2O. PCR was performed for 23 cycles for L32 and 40–45 cycles for other primer pairs, such that all products could be assayed in the exponential phase of the amplification curve, in a thermal cycler (ASTTEC Program Temp Control System PC-800). After an initial step at 94°C for 5 minutes to activate the polymerase, each cycle consisted of 0.5 minutes denaturation at 95°C and 0.5 minutes annealing at the following temperatures: VEGF, 55°C 42cycles; Flt-1, 60°C 42 cycles; IL-1 α, 59°C 42 cycles; TNF-α, 57°C 40 cycles; IL-6, 60°C 42 cycles; and RANKL, 56°C 45 cycles. This was followed by a 0.5-minute extension at 72°C. Products were separated by electrophoreses on 1.5% agarose gels and visualized by staining with ethidium bromide. The luminescence was determined with a charge-coupled device image sensor (ATTO, Tokyo, Japan). For determination of initial levels of templates, the regression equation $y = a \times b^n$, where y is the luminescence and n is the number of cycles, was fitted to the data in the linear portion of semilogarithmic graphs.[21] The constants a and b of the equation are the amounts of original templates and the efficiency of amplification for each cycle, respectively. L32 was used as an internal control.

Statistical analysis

Means of groups were compared by ANOVA, and significance of differences was determined by post hoc testing using Bonferroni's method. Differences were considered significant for $p < 0.05$. Data are presented as mean ± SE.

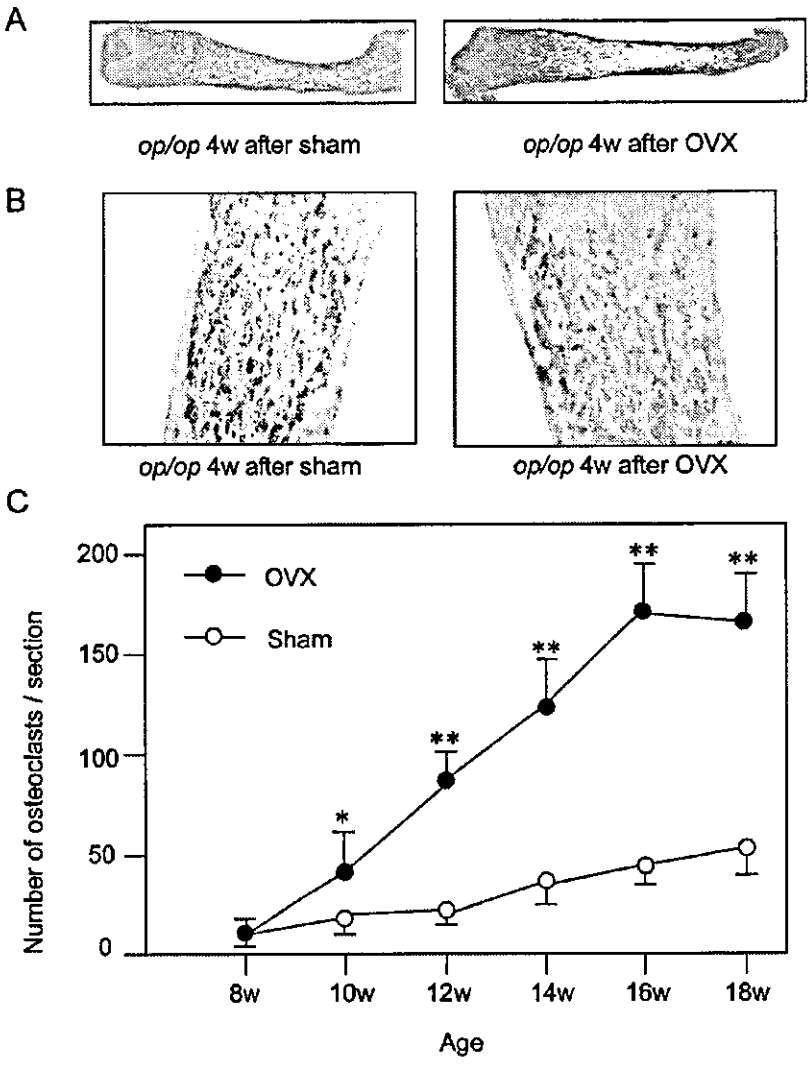

FIG. 1. OVX induces osteoclastic bone resorption in *op/op* mice. (A) Histological finds by AZAN staining at 8 weeks after operation. (B) Histological findings by TRACP staining at 4 weeks after surgery. (C) Osteoclast number after operation. Data are expresed as means ± SEM (error bars). $*p < 0.05$; $**p < 0.01$ vs. Sham.

RESULTS

OVX induces osteoclast formation in M-CSF–deficient op/op *mice*

In sham-operated mice, bone structure was not changed, and the trabecular bone volume of the femur decreased gradually over time. In OVX mice, bone structure was changed, as shown as Fig. 1A, and femoral trabecular bone volume was decreased. Vessels in bone tissue that were immunostained with CD31 increased in OVX mice, corresponding to the increase of bone marrow area, but there were no significant changes in vasculature between OVX mice and sham-operated mice (data not shown). The number of $TRACP^+$ osteoclasts was significantly increased ($p < 0.05$) in OVX mice 2 weeks after surgery and reached a plateau at 8 weeks after OVX (four times the number of osteoclasts as seen in sham-operated mice) despite the absence of functional M-CSF secretion (Figs. 1B and 1C).

Serum levels of VEGF and VEGF mRNA levels in bone tissue increased in a estrogen-deficient condition

It was expected that the increase in osteoclast number was dependent on accelerated VEGF production. Thus, we sought to measure serum levels of VEGF and steady-state levels of VEGF mRNA in bone tissue. In this study, serum levels of VEGF were elevated ($p < 0.05$) in OVX mice compared with sham-operated mice, but no significant differences were observed in serum levels of IL-1 α and TNF-α between OVX mice and sham-operated mice (Fig. 2). At 2 weeks after operation, serum levels of VEGF were elevated ($p < 0.05$) in OVX mice (93.0 ± 11.3 pg/ml) compared with sham-operated mice (62.3 ± 10.9 pg/ml). Levels of VEGF, RANKL, IL-6, and Flt-1 mRNA were elevated ($p < 0.05$) in OVX mice compared with sham-operated mice 4 weeks after the operation, but no significant differences were seen in mRNA levels of IL-1 α and TNF-α between OVX mice and sham-operated mice (Fig. 3).

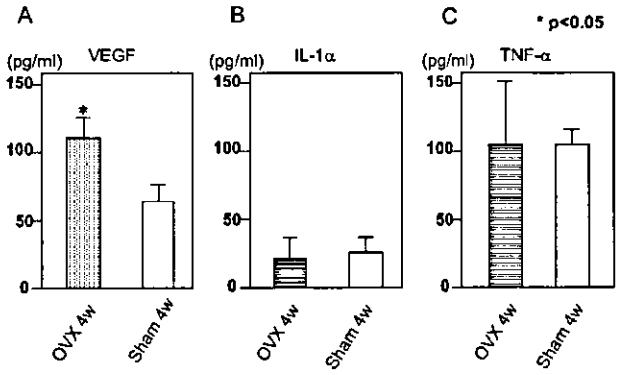

FIG. 2. Serum levels of VEGF increased in the estrogen-deficient condition. (A) Serum levels of VEGF were elevated in OVX mice compared with sham-operated mice. *$p < 0.05$ vs. Sham. (B and C) No significant differences were seen in serum levels of IL-1α and TNF-α between OVX mice and sham-operated mice. Data are expresses as means ± SEM (error bars).

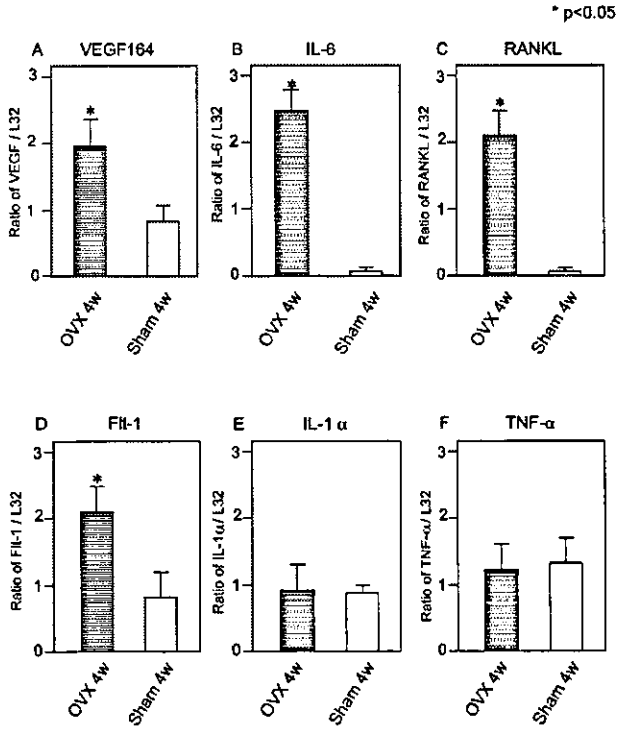

FIG. 3. VEGF, IL-6, RANKL, and Flt-1 mRNA levels in bone tissue increased in the estrogen-deficient condition. (A–D) mRNA levels of VEGF, IL-6, RANKL, and Flt-1 were increased in OVX mice compared with sham-operated mice. *$p < 0.05$ vs. Sham. (E and F) No significant differences were seen in mRNA levels of IL-1α and TNF-α between OVX mice and sham-operated mice. Data are expressed as means ± SEM (error bars).

VEGF antagonistic treatment suppressed the increase of osteoclast number induced by estrogen deficiency in op/op *mice*

Treatment of OVX mice from the time of surgery with VEGFR-1/Fc chimeric protein or 17β-estradiol significantly ($p < 0.05$) suppressed the increase of osteoclast number induced by estrogen deficiency (VEGF antagonistic treatment study 1; Fig. 4). Subcutaneous injection of OVX mice with VEGF neutralizing antibody every 12, 24, and 36 h before death significantly suppressed the estrogen deficiency–induced increase in osteoclast number (VEGF antagonistic study 2; Fig. 5).

DISCUSSION

The four major findings of this study are (1) OVX-induced estrogen deficiency induces osteoclast formation and cures osteopetrosis in M-CSF deficient *op/op* mice; (2) serum levels of VEGF were elevated in OVX mice compared with sham-operated mice; (3) steady-state levels of VEGF, RANKL, IL-6, and Flt-1 mRNA in bone tissue were elevated in OVX mice compared with sham-operated mice 4 weeks after the operation; and (4) VEGF acts as a factor promoting osteoclast differentiation and survival in *op/op* mice.

This is the first report that shows that OVX-induced estrogen deficiency induces osteoclast formation by increases of steady-state VEGF levels in bone tissue.

OVX-induced estrogen deficiency induces osteoclast formation and cures osteopetrosis in M-CSF–deficient op/op *mice*

In several previous studies, the mechanisms of estrogen deficiency induced increase in bone resorption and were discussed for mice with normal M-CSF production.[22–24] We now show that the estrogen deficiency–induced increase in bone resorption was seen in mice incapable of producing functional M-CSF. Previous studies have reported that OVX induces osteoclastic bone resorption in *op/op* mice,[25] but there were no mentions about its mechanisms. We have previously demonstrated,[13] in an osteopetrotic mouse (*op/op* mouse) model, that VEGF replaced M-CSF in support of in vitro and in vivo osteoclast differentiation and acted through Flt-1. It has more recently been demonstrated that VEGF directly enhances osteoclastic bone resorption and the survival of mature osteoclast through VEGF receptors, KDR/Flk-1 and/or Flt-1, expressed in mature osteoclasts.[26] Therefore, it was expected that the increase in osteoclast number was dependent on accelerated VEGF production. Thus, we sought to measure serum levels of VEGF.

Serum levels of VEGF were elevated in OVX mice compared with sham-operated mice

The serum concentration of VEGF in OVX mice was significantly higher than levels seen in sham-operated mice. Also, Sumino et al.[27] have reported that serum VEGF is increased by the atherosclerotic process in postmenopausal women, and it is decreased by hormone replacement therapy (HRT). Several studies reported that estrogen deficiency increases IL-1α activity rather than the amount.[28,29] Zheng et al.[30] have reported that TNF-α production were significantly higher in postmenopausal osteoporotic women. IL-1α and TNF-α are mainly produced by bone marrow mononuclear cells.[5] Because *op/op* mice have few mono-

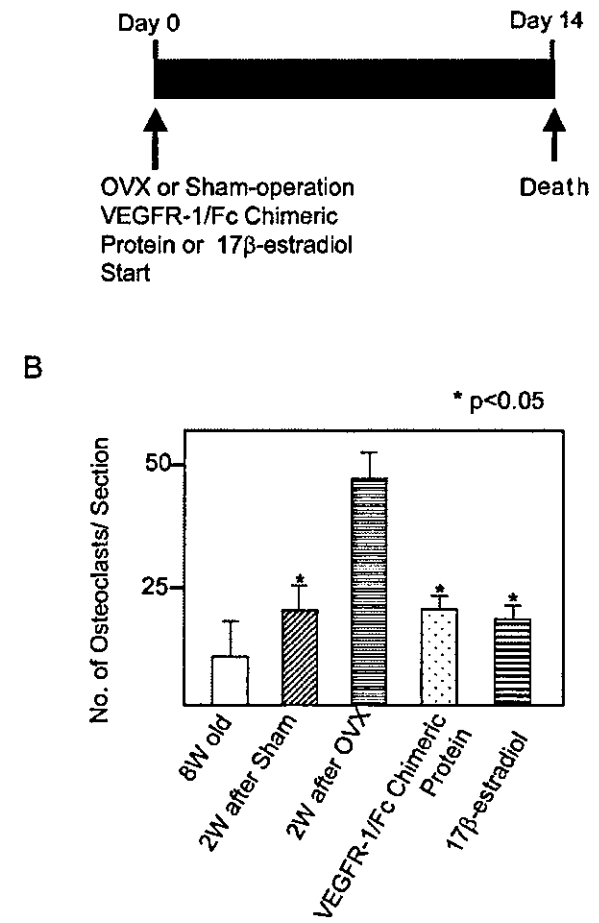

FIG. 4. (A) Design of VEGF antagonistic treatment study 1. (B) Both EGFR-1/Fc chimeric protein and 17β-estradiol initiated at the time of OVX significantly suppressed the increase in osteoclast number ($p < 0.05$ vs. 2 weeks after OVX) induced by estrogen deficiency. Data are expressed as means ± SEM (error bars).

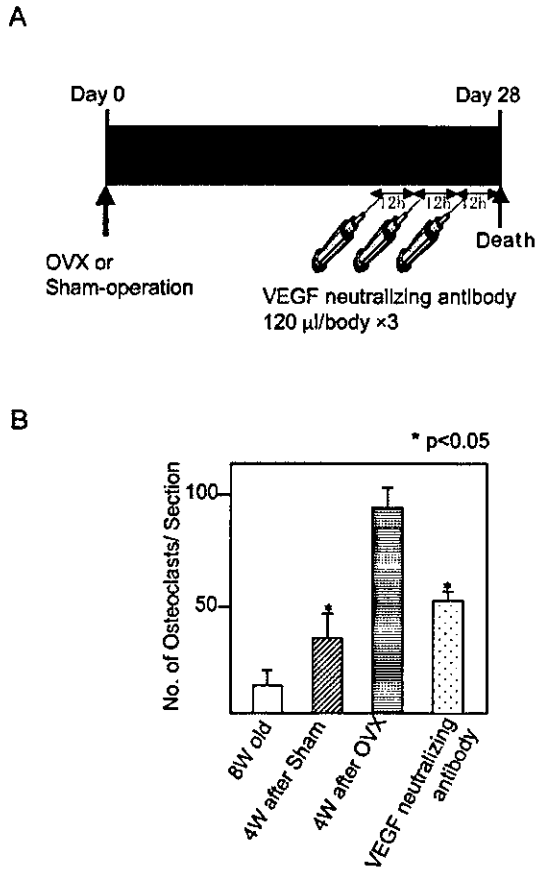

FIG. 5. (A) Design of VEGF antagonistic treatment study 2. (B) VEGF neutralizing antibody administered to OVX mice every 12, 24, and 36 h before death significantly suppressed the estrogen deficiency–induced increase in osteoclasts ($p < 0.05$ vs. 4 weeks after OVX). Data are expressed as means ± SEM (error bars).

cytes, these results can be accepted. These results indicate that the increase of VEGF production may induce osteoclast formation.

Levels of VEGF, RANKL, IL-6, and Flt-1 mRNA were elevated in OVX mice compared with sham-operated mice 4 weeks after operation

To examine whether steady-state levels of VEGF mRNA in bone tissue are elevated and what promotes the VEGF production in OVX *op/op* mice, we sought to measure VEGF, RANKL, IL-6, Flt-1, IL-1α, and TNF-α mRNA by semiquantitative RT-PCR. Results from RT-PCR show that steady-state levels of VEGF mRNA, RANKL mRNA, Flt-1 mRNA, and IL-6 mRNA in bone tissue are elevated in OVX *op/op* mice. VEGF is a potent stimulator of angiogenesis and a prognostic factor for many tumors, including those of endocrine-responsive tissues such as the breast and uterus.[31,32] Although VEGF is secreted by many cell types in the skeleton, osteoblasts and chondrocytes have been reported to produce this cytokine.[33,34] A number of cytokines, hormones, and growth factors are able to upregulate VEGF mRNA expression in various cell types,[35] but less is known about the role of estradiol in VEGF regulation. It has previously been shown that VEGF is regulated by estradiol and tamoxifen in the uterus and by estradiol in human breast cancer cells, and pharmacologic evidence has suggested that this regulation is mediated by transcriptional activation of the estrogen receptor (ER).[36] Results from RT-PCR have shown that estrogen deficiency may induce the production of VEGF by an increase in IL-6 production in bone tissue. IL-6 has been shown to significantly induce VEGF expression in several cell lines.[33]

Conversely, hypoxia is key regulator of VEGF gene expression, both in vitro and in vivo.[37,38] Recently, Steinbrech et al.[39] have shown that hypoxia specifically and potently regulates the expression of VEGF by osteoblasts. We previously reported that estrogen deficiency leads to a decrease in the serum levels of nitric oxide (NO) and that estrogen replacement therapy increases serum levels of NO.[40] These findings indicate the possibility that estrogen deficiency may cause the hypoxia in several organs through a decrease of NO.[41] This hypothesis is further supported

by previous studies that have shown that NO donor therapy can prevent OVX-induced bone loss.[42,43]

VEGF acts as a factor promoting osteoclast differentiation and survival in op/op *mice*

Finally, we used VEGF antagonists to further reinforce the role of VEGF in osteoclast function. Results from VEGF antagonistic treatment study 1 indicate that VEGF functions as a factor promoting osteoclast differentiation in M-CSF–deficient OVX *op/op* mice. Results from VEGF antagonistic study 2 indicate that VEGF functions as a survival factor for osteoclasts, because the number of osteoclasts were increased directly before VEGF neutralizing antibody treatment.

In summary, treatment of mice with VEGF antagonists showed that VEGF enhances osteoclast formation and the survival of mature osteoclasts in the estrogen-deficient condition. And these are in vivo supporting data for recent in vitro study data showing that VEGF directly enhances osteoclast formation and survival of mature osteoclasts through activation of VEGF receptors, KDR/Flk-1 and/or Flt-1, expressed in mature osteoclasts.[26]

Taken together, these results indicate that VEGF is an important regulator of osteoclastic bone resorption in *op/op* mice. There is a possibility that VEGF regulates osteoclastic bone resorption mainly caused by estrogen deficiency even in mice with normal M-CSF production, but more research needs to be done to prove it.

In conclusion, we now report that estrogen deficiency induces osteoclastic bone loss in *op/op* mice through an increase in VEGF production in bone tissue.

ACKNOWLEDGMENTS

The authors thank the Experimental Animal Center of Hiroshima University for assistance of animal care. We also thank T Okamura and S Hiyama for technical comments. This work was supported, in part, by a Grant-in-Aid for Scientific Research 12671772 and 14770852 from the Ministry of Education, Culture, Sports, Science and Technology of Japan (SN and IK), a Research Grant for Longevity Sciences (14A-2) from the Ministry of Health, Labour and Welfare (SN), and a grant from Kanzawa Medical Research Foundation (SN).

REFERENCES

1. Manolagas SC, Jilka RL 1995 Bone marrow, cytokines, and bone remodeling. N Engl J Med **332:**305–311.
2. Tanaka S, Takahashi N, Udagawa N, Tamura T, Akatsu T, Stanley FR, Kurokawa T, Suda T 1993 Macrophage colony-stimulating factor is indispensable for both proliferation and differentiation of osteoclast progenitors. J Clin Invest **91:**257–263.
3. Dexter TM, Allen TD, Lajtha LG 1977 Conditions controlling the proliferation of haemopoietic stem cells in vitro. J Cell Physiol **91:**335–344
4. Chaplin DD, Hogqist K 1992 Tumor necrosis factors. In:Beutler B (ed.) The Molecules and Their Emerging Role in Medicine. Raven Press, New York, NY, USA, pp. 197–220.
5. Pfeilschifter J, Chenu C, Bird A, Mundy GR, Roodman GD 1989 Interleukin-1 and tumor necrosis factor stimulate the formation of human osteoclastlike cells in vitro. J Bone Miner Res **4:**113–118.
6. van der Pluijm G, Most W, van der Wee-Pals L, de Groot H, Papapoulos S, Lowik C 1991 Two distinct effects of recombinant human tumor necrosis factor-alpha o n osteoclast development and subsequent resorption of mineralized matrix. Endocrinology **129:** 1596–1604.
7. Matsuzaki K, Udagawa N, Takahashi N, Yamaguchi K, Yasuda H, Shima N, Morinaga T, Toyama Y, Yabe Y, Higashio K, Suda T 1998 Osteoclast differentiation factor (ODF) induces osteoclast-like formation in human peripheral blood mononuclear cell cultures. Biochem Biophys Res Commun **246:**199–204.
8. Wong BR, Rho J, Arron J, Robinson E, Orlinick J, Chao M, Kalachikov S, Cayani E, Bartlett FS, Frankel WN, Lee SY, Choi Y 1997 TRANCE is a novel ligand of the tumor necrosis factor receptor family that activates c-Jun N-terminal kinase in T cells. J Biol Chem **272:**25190–25194.
9. Marks SCJ 1982 Morphological evidence of reduced bone resorption in osteopetrotic (*op*) mice. Am J Anat **163:**157–167.
10. Wiktor-Jedrzejczak W, Ahmed A, Szczylik C, Skelly RR 1982 Hematological characterization of congenital osteopetrosis in *op/op* mouse. J Exp Med **156:**1516–1527.
11. Begg SK, Radley JM, Polland JW, Chisholm OT, Stanley ER, Bertoncello I 1993 Delayed hematopoietic development in osteopetrotic (*op/op*) mice. J Exp Med **177:**237–242.
12. Niida S, Kaku M, Amano H, Yoshida H, Kataoka H, Nishikawa S, Tanne K, Maeda N, Nishikawa N, Kodama H 1999 Vascular endothelial growth factor can substitute for macrophage colony-stimulating factor in the support of osteoclastic bone resorption. J Exp Med **190:**293–298.
13. Kodama H, Yamasaki A, Nose M, Niida S, Ohgae Y, Abe M, Kumegawa M, Suda T 1991 Congenital osteoclast deficiency in osteopetrotic (*op/op*) mice is cured by injections of macrophage colony-stimulating factor. J Exp Med **173:**269–272.
14. Kodama H, Yamasaki A, Abe M, Niida S, Hakeda Y, Kawashima H 1993 Transient recruitment of osteoclasts and expression of their function in osteopetrotic (*op/op*) mice by a single injection of macrophage colony-stimulating factor. J Bone Miner Res **8:**45–50.
15. Niida S, Amizuka N, Hara F, Ozawa H, Kodama H 1994 Expression of Mac-2 antigen in the preosteoclast and osteoclast identified in the *op/op* mouse injected with macrophage colony-stimulating factor. J Bone Miner Res **9:**873–881.
16. Tober KL, Cannon RE, Spalding JW, Oberyszyn TM, Parrett ML, Rackoff AI, Oberyszyn AS, Tennant RW, Robertson FM 1998 Comparative expression of novel vascular endothelial growth factor/vascular permeability factor transcripts in skin, papillomas, and carcinomas of v-Ha-ras Tg. AC transgenic mice and FVB/N mice. Biochem Biophys Res Commun **247:**644–653.
17. He Y, Smith SK, Day KA, Clark DE, Licence DR, Charnock-Jones DS 1999 Alternative splicing of vascular endothelial growth factor (VEGF)-R1 (FLT-1) pre-mRNA is important for the regulation of VEGF activity. Mol Endocrinol **13:**537–545.
18. Haynes DR, Atkins GJ, Loric M, Crotti TN, Geary SM, Findlay DM 1999 Bidirectional signaling between stromal and haemopoietic cells regulates interleukin-1 expression during human osteoclast formation. Bone **25:**269–278.
19. Ulett GC, Ketheesan N, Hirst R 2000 Cytokine gene expression in innately susceptible BALB/c mice and relatively resistant C57BL/6 mice during infection with virulent Burkholderia pseudomallei. Infect Immun **68:**2034–2042.
20. Atkins GJ, Haynes DR, Geary SM, Loric M, Crotti TN, Findlay DM 2000 Coordinated cytokine expression by stromal and hematopoietic cells during human osteoclast formation. Bone **26:**653–661.
21. Yokoi H, Natsuyama S, Iwai M, Noda Y, Mori T, Mori J, Fujita K, Nakayama H, Fujita J 1993 Non-radioisotropic quantitative RT-PCR to detect changes in mRNA levels during early mouse embryo development. Biochem Biophys Res Commun **195:**769–775.
22. Kimble R, Srivastava S, Ross F, Matayoshi A, Pacifici R 1996 Estrogen deficiency increases the ability of stromal cells to support murine osteoclastogenesis via an interleukin-1 and tumor necrosis factor-mediated stimulation of macrophage colony-stimulating factor production. J Biol Chem **271:**28890–28897.
23. Kitazawa R, Kimble R, Vannice J, Kung V, Pacifici R 1994 Interleukin-1 receptor antagonist and tumor necrosis factor binding protein decrease osteoclast formation and bone resorption in ovariectomized mice. J Clin Invest **94:**2397–2406.
24. Srivastava S, Weitzmann M, Kimble R, Rizzo M, Zahner M, Milbrandt J, Ross F, Pacifici R 1998 Estrogen blocks M-CSF gene expression and osteoclast formation by regulating phosphorylation of Egr-1 and its interaction with Sp-1. J Clin Invest **102:**1850–1859.

25. Kawata T, Fujita T, Kumegawa M, Tanne K 1999 Congenital osteoclast deficiency in osteopetrotic (*op/op*) mice is improved by ovariectomy and orchiectomy. Exp Anim **48:**125–128.
26. Nakagawa M, Kaneda T, Arakawa T, Morita S, Sato T, Yomada T, Hanada K, Kumegawa M, Hakeda Y 2000 Vascular endothelial growth factor (VEGF) directly enhances osteoclastic bone resorption and survival of mature osteoclasts. FEBS Lett **473:**161–164.
27. Sumino H, Nakamura T, Ichikawa S, Kanda T, Sakamaki T, Sato K, Kobayashi I, Nagai R 2000 Serum level of vascular endothelial growth factor is decreased by hormone replacement therapy in postmenopausal women without hypercholesterolemia. Atherosclerosis **148:**189–195.
28. Miyaura C, Kusano K, Masuzawa T, Chaki O, Onoe Y, Aoyagi M, Sasaki T, Tamura T, Koishihara Y, Ohsugi Y 1995 Endogenous bone-resorbing factors in estrogen deficiency: Cooperative effects of IL-1 and IL-6. J Bone Miner Res **10:**1365–1373.
29. Khosla S, Peterson JM, Egan K, Jones JD, Riggs BL 1994 Circulating cytokine levels in osteoporotic and normal women. J Clin Endocrinol Metab **79:**707–711.
30. Zheng SX, Vrindts Y, Lopez M, De Groote D, Zangerle PF, Collette J, Franchimont N, Geenen V, Albert A, Reginster JY 1997 Increase in cytokine production (IL-1β, IL-6, TNF-α but not IFN-γ, GM-CSF or LIF) by stimulated whole blood cells in postmenopausal osteoporosis. Maturitas **26:**63–71.
31. Hyder SM, Nawaz Z, Chiappetta C, Stancel GM 2000 Identification of functional estrogen response elements in the gene coding for the potent angiogenic factor vascular endothelial growth factor. Cancer Res **60:**3183–3190.
32. Adams J, Carder PJ, Downey S, Forbes MA, MacLennan K, Allgar V, Kaufman S, Hallam S, Bicknell R, Walker JJ, Cairnduff F, Selby PJ, Perren TJ, Lansdown M, Banks RE 2000 Vascular endothelial growth factor (VEGF) in breast cancer: Comparison of plasma, serum, and tissue VEGF and microvessel density and effects of tamoxifen. Cancer Res **60:**2898–2905.
33. Goad DL, Rubin J, Wang H, Tashjian AH Jr, Patterson C 1996 Enhanced expression of vascular endothelial growth factor in human SaOS-2 osteoblast-like cells and murine osteoblasts induced by insulin-like growth factor I. Endocrinology **137:**2262–2268.
34. Gerber HP, Vu TH, Ryan AM, Kowalski J, Werb Z, Ferrara N 1999 VEGF couples hypertrophic cartilage remodeling, ossification and angiogenesis during endochondral bone formation. Nat Med **5:**623–628.
35. Ferrara N 1999 Molecular and biological properties of vascular endothelial growth factor. J Mol Med **77:**527–543.
36. Hyder SM, Stancel GM 2000 Regulation of VEGF in the reproductive tract by sex-steroid hormones. Histol Histopathol **15:**325–334.
37. Minchenko A, Bauer T, Salceda S, Caro J 1994 Hypoxic stimulation of vascular endothelial growth factor expression in vivo and in vitro. Lab Invest **71:**374–379.
38. Shima DT, Adamis AP, Ferrara N, Yeo KT, Yeo TK, Allende R, Folkman J, D'Amore PA 1995 Hypoxic induction of endothelial cell growth factors in retinal cells: Identification and characterization of vascular endothelial growth factor (VEGF) as the mitogen. Mol Med **1:**182–193.
39. Steinbrech D, Mehrara B, Saddeh P, Greenwald J, Spector J, Gittes G, Longaker M 2000 VEGF expression in an osteoblast-like cell line is regulated by a hypoxia response mechanism. Am J Physiol Cell Physiol **278:**C853–C860.
40. Sanada M, Higashi Y, Nakagawa K, Tsuda M, Kodama I, Kimura M, Chayama K, Ohama K 2002 Hormone replacement effects on endothelial function measured in the forearm resistance artery in normocholesterolemic and hypercholesterolemic postmenopausal women. J Clin Endocrinol Metab **87:**4634–4641.
41. Pohl U, Wagner K, de Wit C 1993 Endothelium-derived nitric oxide in the control of tissue perfusion and oxygen supply: Physiological and pathophysiological implications. Eur Heart J **14:**93–98.
42. Wimalawansa SJ 2000 Nitroglycerin therapy is as efficacious as standard estrogen replacement therapy (Premarin) in prevention of oophorectomy-induced bone loss: A human pilot study. J Bone Miner Res **15:**2240–2244.
43. Wimalawansa SJ, De Marco G, Gangula P, Yallampalli C 1996 Nitric oxide donor alleviates ovariectomy-induced bone loss. Bone **18:**301–304.

Address reprint requests to:
Ichiro Kodama, MD
Department of Obstetrics and Gynecology
Graduate School of Biomedical Sciences
Hiroshima University
1-2-3, Kasumi, Minami-ku
Hiroshima City 734-8551, Japan
E-mail: ikodama@hiroshima-u.ac.jp

Received in original form May 8, 2003; in revised form August 29, 2003; accepted September 11, 2003.

Journal of the American College of Cardiology
© 2004 by the American College of Cardiology Foundation
Published by Elsevier Inc.

Vol. 43, No. 5, 2004
ISSN 0735-1097/04/$30.00
doi:10.1016/j.jacc.2003.08.060

Matrix Metalloproteinase-9 Contributes to Human Atrial Remodeling During Atrial Fibrillation

Yukiko Nakano, MD,* Shumpei Niida, PHD,† Keigo Dote, MD,‡ Sou Takenaka, MD,* Hidekazu Hirao, MD,* Fumiharu Miura, MD,* Mari Ishida, MD,* Tetsuji Shingu, MD,* Taijiro Sueda, MD,§ Masao Yoshizumi, MD,‖ Kazuaki Chayama, MD*

Hiroshima and Nagoya, Japan

OBJECTIVES The purpose of this study was to determine the relationship between matrix metalloproteinases (MMPs)-1, -2, and -9, and tissue inhibitors of metalloproteinases (TIMP)-1 and the atrial structural remodeling during atrial fibrillation (AF).

BACKGROUND Matrix metalloproteinases, a family of proteolytic enzymes and TIMPs, regulate the extracellular matrix turnover in cardiac tissue.

METHODS Tissue samples were obtained from 25 patients without a history of AF (regular sinus rhythm [RSR]) and 13 patients with AF (paroxysmal AF: 6, chronic AF 7) undergoing cardiac operations. We performed a western blotting analysis of the MMP-1, -2, and -9, and quantitatively analyzed the expression of the MMP-9 and TIMP-1 by real time polymerase chain reaction and ELISA. The localization of the MMP-9 was investigated by in situ zymography and immunohistochemistry.

RESULTS The active form of the MMP-9 was significantly increased in the AF group in comparison to that in the RSR group ($p < 0.05$), but there were no differences between the groups in the protein level of the latent form of the MMP-9 and active and latent forms of the MMP-1 and MMP-2. We also demonstrated that the expression of the MMP-9 was significantly more increased in the atria of the AF group than in that of the RSR group for both the messenger ribonucleic acid (mRNA) (AF: RSR; 1: 1.5) and protein levels (AF: RSR; $3.9 \pm 1.3 : 1.5 \pm 0.4$ ng/mg atrium). The expression level of the MMP-9 was also higher in the PAF group than in the RSR group, however, the diameter of the left atrium was similar in both groups. The gelatinase activity and left atrium diameter were positively correlated ($p < 0.05$, $R = 0.766$). The relative expression of the mRNA for the monocyte chemoattractant protein-1 was higher in the AF group than in the RSR group. Immunohistochemical analysis revealed that the MMP-9 was distributed within the perivascular area and under the epicardium of the atria.

CONCLUSIONS We clearly showed that the expression of the MMP-9 increased in fibrillating atrial tissue, which may have contributed to the atrial structural remodeling and atrial dilatation during AF. (J Am Coll Cardiol 2004;43:818–25) © 2004 by the American College of Cardiology Foundation

Atrial fibrillation (AF) is the most common arrhythmia (1) and is well known as a source of thromboembolic events (2). The longer the duration of AF, the more persistent it becomes because of atrial remodeling. A shortening of the atrial refractory period, termed "electrical remodeling" (3–7), occurs first. Then, contractile remodeling, meaning a decrease in the atrial contractility, occurs, followed by structural remodeling, which guarantees the persistence of AF (8,9). Several reports have demonstrated that electrical remodeling was caused by a reduction in the L-type Ca^{2+} channels and various kinds of potassium channels in atria with AF (10–13). However, both the mechanism and the role of the structural remodeling of AF still remain unclear. Remodeling of cellular ultrastructures, such as myolysis occurring in the atrial myocardium, is known to develop progressively during AF (14). An increase in the expression of the gap junctions (connexin 40) has been reported to induce changes in the biophysical properties of the atrial tissue during AF (15,16). Enhanced disintegrin and metalloproteinase (ADAM) activity was also reported to be a molecular mechanism contributing to the dilation of fibrillating human atria (17).

Matrix metalloproteinases (MMPs) are a family of proteolytic enzymes, and they regulate the extracellular matrix turnover in a balance with the tissue inhibitors of metalloproteinases (TIMPs) (18,19). The extracellular matrix degradation by MMPs has been known to be associated with the pathogenesis of cardiovascular diseases, including atherosclerosis, restenosis, dilated cardiomyopathy, and myocardial infarction (MI) (20,21). In particular, many reports have demonstrated that MMP-9

From the *Department of Medicine and Molecular Science, Graduate School of Biomedical Science, Hiroshima University, Hiroshima, Japan; †Department of Geriatric Research, National Institute for Longevity Science (NILS), Nagoya, Japan; ‡Department of Cardiology, Hiroshima City Asa Hospital, Hiroshima, Japan; §Department of Surgery, Hiroshima Graduate School of Medicine, Graduate School of Biomedical Science, Hiroshima University, Hiroshima, Japan; and ‖Department of Cardiovascular Physiology and Medicine, Graduate School of Biomedical Science, Hiroshima University, Hiroshima, Japan. This work was supported by the Tsuchiya Heart Foundation and Kimura Memorial Heart Foundation.

Manuscript received July 2, 2003; revised manuscript received July 28, 2003, accepted August 5, 2003.

Abbreviations and Acronyms

AF	= atrial fibrillation
ADAM	= A Disintegrin And Metalloproteinase
MCP-1	= monocyte chemoattractant protein-1
MMPs	= matrix metalloproteinases
PAF	= paroxysmal AF
RSR	= regular sinus rhythm
RT-PCR	= reverse transcription-polymerase chain reaction
TIMPs	= tissue inhibitors of metalloproteinases

plays an important role in ischemia-reperfusion–induced myocardial matrix remodeling and could be a target for the prevention or treatment of acute ischemic myocardial injury (19,21–25).

The purpose of this study was to investigate the role of MMP-1, -2, and -9 and TIMP-1 in AF-induced human atrial remodeling.

METHODS

Tissue collection. Right atrial appendages were obtained from 38 patients undergoing cardiac operations, which consisted of 25 patients with regular sinus rhythm (RSR) without a history of AF, and 13 patients with AF (paroxysmal AF [PAF]: 6 patients; chronic AF [CAF]: 7 patients). The institutional ethics committee of the Graduate School of Biomedical Science, Hiroshima University, approved all procedures involving human tissue usage. Informed consent was obtained from patients before tissue harvesting. A transverse section (5 to 8 mm) of the atrial appendage was divided into three sections. One was embedded in an OCT compound (Sakura, Torrance, California) and frozen with liquid nitrogen. The tissue blocks were stored at −80°C until sectioning. Another section was quickly frozen with liquid nitrogen and stored at −80°C until the protein would be extracted. The other section was preserved in RNAlater (Ambion, Austin, Texas) at 4°C and used to extract the RNA.

ELISA and Western blotting analysis. Frozen cardiac samples were homogenized in a lysis buffer (20 mmol/l Tris; 1% Triton X; 10% glycerol; 1% DOC; 0.1% SDS; 50 mmol/l NaF; 10 mmol/l NaP_2O_4; 1 mmol/l DTT; 1 mmol/l Banadate; 10 μg/ml leupeptin, pH 7.4) with a Zilconia bead at 30 frequency/s and 4°C for 8 min using an MM 300 (Quagen, Hilden, Germany) and centrifuged at 14,000 rpm at 4°C for 10 min. The protein concentrations of the supernatants were determined by DC protein assay (Bio-Rad, Richmond, California). Equal amounts of the proteins were assayed for human MMP-9 and TIMP-1 production by ELISA kits purchased from R&D Systems (Minneapolis, Minnesota) according to the manufacturer's instructions. All assays were performed in duplicate.

The same samples used for the ELISA assay of the MMP-9 were also used for the Western blot analysis of the MMP-1, -2, and -9. Equal amounts of protein (2 μg) were separated by SDS–PAGE and immunoblotted to a nitrocellulose membrane with anti-MMP antibodies (Oncogene Research Products, San Diego, California), which recognized their latent or active forms. The MMP protein bands were visualized using HRP-conjugated anti-IgG secondary antibodies and ECL plus Western blotting detection reagents (Amersham Biosciences, Buckinghamshire, UK). The membranes were washed, dried, and exposed to X-ray film (Kodak). The images were analyzed with National Institutes of Health (NIH) images and quantified by normalizing them with that from beta-actin.

Quantitative reverse transcription-polymerase chain reaction (RT-PCR). Tissue samples taken from the RNAlater (Ambion, Austin, Texas) were pulverized in Trizol reagents (1 ml/100 mg tissue), and the total RNA was extracted by the Trizol method supplied by Invitrogen. Precisely 1 μg of the total RNA from each sample was reverse-transcribed to generate complementary deoxyribonucleic acid (cDNA) using Ready-To-Go RT-PCR beads (Amersham Pharmacia, Piscataway, New Jersey) and the random primer *pd (N)6*. This mixture was placed in a thermal cycler (model 9600) at 42°C for 20 min and 95°C for 5 min. Quantitative PCR was performed using a Light Cycler (Roche, Mannheim, Germany). The cDNA (10 μl each) was diluted to a volume of 20 ml with a PCR mixture (Light Cycler Fast Start DNA Master SYBR Green I kit [Roche]) containing 0.5 μmol of specific primers (Light Cycle Primer Set) for the MMP-9, TIMP-1, monocyte chemoattractant proteins (MCP-1), and tumor necrosis factor-alpha (TNF-α). Initial denaturation at 95°C for 10 m was followed by amplification, involving 35 cycles with denaturation at 95°C for 10 m, annealing at 68°C for 10 s and elongation at 72°C for 16 s. All samples were analyzed in triplicate. The fluorescence intensity of the SYBR Green I reflected the amount of PCR products actually formed.

Film in situ zymography. In situ zymography using FIZ films was used to determine the localization of the MMP-2, -3, -7, and -9 activity. The FIZ films were coated with gelatin in either the presence (FIZ-GI film) or absence (FIZ-GN film) of an MMP inhibitor (1,10-phenanthroline) (FUJIFILM, Japan). Unfixed frozen sections (6 μm) were placed on the films and incubated for 24 h at 37°C with 100% humidity and stained with Biebrich scarlet. The MMP-2, -3, -7, and -9 activity was visualized by both the loss of staining in the FIZ-GN films and staining in the FIZ-GI films. Images of the FIZ-GN films were scanned, and the gelatinase activity was analyzed using NIH images.

Immunohistochemical staining of MMP-9 and CD11b. We conducted double immunofluorescent staining for MMP-9 (Santa Cruz, California) and CD11b (macrophage marker, Dako Japan, Kyoto). The nuclei were stained with Hoechst 33342. Frozen sections of atrium were washed with PBS, fixed with 4% paraformaldehyde for 15 min at room temperature, and permeabilized with 0.5% Triton X-100/PBS for 5 min. After blocking with 1% BSA/PBS

Table 1. LV Function and LV Mass Among AF and RSR Groups

	AF (n = 13)	RSR (n = 25)
Gender (male/female)	10/3	20/5
Age (yrs)	68 ± 9	65 ± 12
Echocardiography		
LAD (mm)	50.6 ± 9.2*	35.7 ± 6.1
IVSTd (mm)	11.2 ± 2.5	10.8 ± 2.4
LVDd (mm)	52.8 ± 9.5	48.2 ± 7.5
EF (%)	58.1 ± 5.0	61.3 ± 16.9
Medication		
ACE inhibitor (%)	23	8
ARB (%)	8	4
Digoxin (%)	62*	8
Diuretics (%)	38	32
Beta-blocker (%)	15	12
Ca-blocker (%)	15*	60
Nitrate (%)	8*	56
Operation (%)		
CABG	8	77
Valve (A/M/T)	54 (8/61/15)	23 (8/12/4)
Thrombotectomy	54	0
Maze	31	0

*p = 0.05, atrial fibrillation vs. regular sinus rhythm.

A = aortic valve; AF = atrial fibrillation; ARB = angiotensin II receptor blocker; EF = ejection fraction; IVSTd = interventricular septum thickness; LAD = left atrial diameter; LV = left ventricular; LVDd = left ventricle diastolic diameter; M = mitral valve; RSR = regular sinus rhythm; T = tricuspid valve; Thrombectomy = left atrial or left atrial appendages thrombectomy; Valve (A/M/T) = valve replacement or plasty.

and incubating with primary antibodies in 1% BSA/PBS, the sections were incubated with secondary antibodies (Alexa 488/568). Specimens were observed using confocal laser scanning microscopy (Leica DM IRBE).

Statistical analysis. Clinical characteristics and quantitative data were compared between the AF and RSR groups by the Mann-Whitney *U* test. The Kruskal-Wallis test was used to compare the three groups (RSR, PAF, and CAF). Data are presented as mean ± SD. A p value < 0.05 was considered statistically significant.

RESULTS

No differences existed in the gender, age, or percentage of oral administration with angiotensin-converting enzyme (ACE) inhibitors, angiotensin I receptor blockers, diuretics, and beta-blockers between the AF and RSR groups. From the cardiac echocardiography, the left ventricular (LV) function and LV mass were similar among the AF and RSR groups (Table 1). The left atrial diameter was similar in the RSR and PAF groups, but larger in the CAF group than in the RSR group (35.7 ± 6.1 mm in the RSR group, 40.2 ± 4.8 mm in the PAF group, and 51.8 ± 10.5 mm in the CAF group, p < 0.05).

As a result of Western blotting analysis, the active form of the MMP-9 (88 kDa) was significantly increased in the AF group in comparison to that in the RSR group (p < 0.05), but no difference existed in the protein level of the latent form (92 kDa) of the MMP-9 and active and latent forms of the MMP-1 (43 and 55 kDa, respectively) and MMP-2 (66 and 72 kDa, respectively) between the two groups (Fig. 1). Also, the ELISA analysis showed that the protein level of the MMP-9 was significantly increased in the AF group in comparison to that in the RSR group (Fig. 2A, p < 0.05).

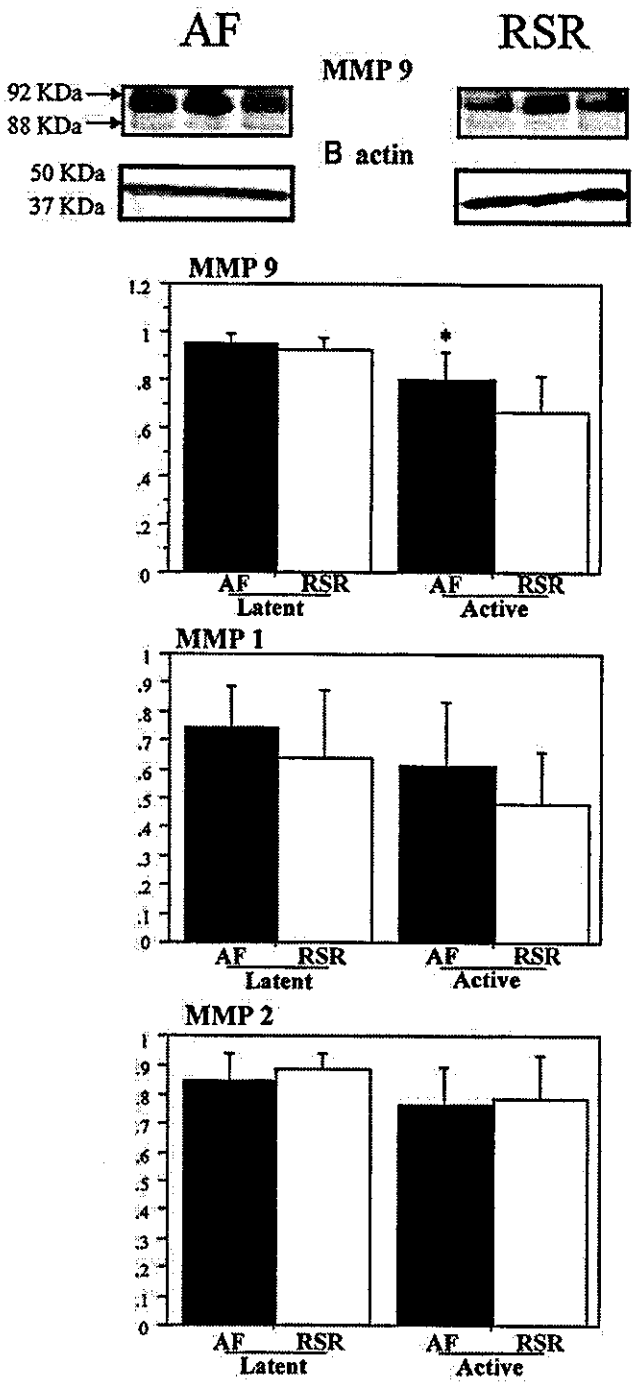

Figure 1. Results of the measurement of the matrix metalloproteinase (MMP)-1, -2, and -9 using the Western blotting analysis. The active form of MMP-9 (88 kDa) significantly increased in the atrial fibrillation (AF) group in comparison to that in the regular sinus rhythm (RSR) group (p < 0.05), but there was no difference in the protein level of the latent form of MMP-9 (92 kDa) **(top panel)**. No difference existed in the protein level of the active and latent forms of the MMP-1 **(middle panel)** and MMP-2 **(bottom panel)** between the two groups. **Closed bars** = AF group; **open bars** = RSR group. *p < 0.05, AF vs. RSR.

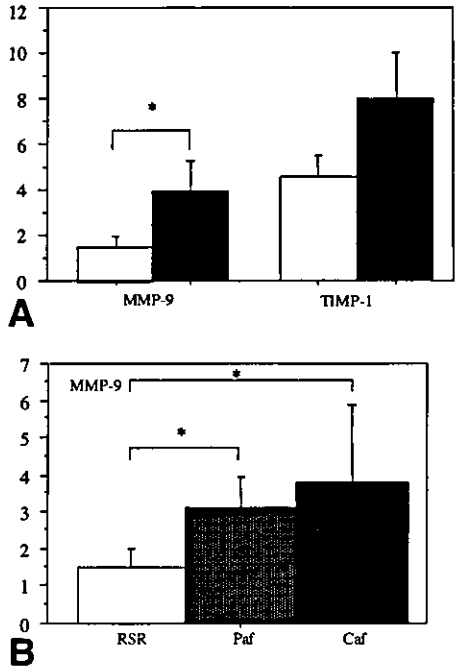

Figure 2. Expression level of the MMP-9 protein and tissue inhibitors of metalloproteinase (TIMP)-1 protein by enzyme-linked immunosorbent assay. **(A)** The expression level of the MMP-9 protein was also higher in the AF group **(closed bar)** than in the RSR group **(open bar)** ($p < 0.05$), and the TIMP-1 protein showed a tendency to rise in the AF patients as compared to that in the RSR patients ($p < 0.1$). **(B)** Comparison of the expression of the MMP-9 protein among the three groups. The expression level of MMP-9 was higher not only in the CAF group, but also in the paroxysmal atrial fibrillation (Paf) group, than that in the RSR group. **Closed bars** = AF group; **open bars** = RSR group. *$p < 0.05$, AF vs. RSR. Abbreviations as in Figure 1.

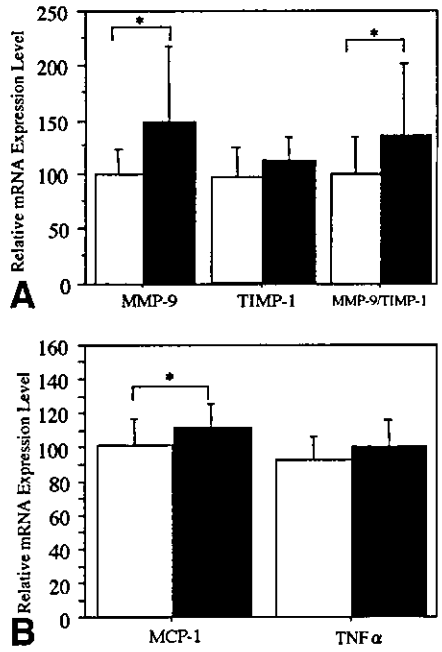

Figure 3. Relative expression of messenger ribonucleic acid (mRNA) from MMP-9, TIMP-1, monocyte chemoattractant protein (MCP)-1, and tumor necrosis factor (TNF-α). **(A)** The relative expression of mRNA from MMP-9 was higher in the AF group than in the RSR group. **(B)** The relative expression of mRNA from MCP-1 was higher in the AF group than in the RSR group and that of the TNF-α was similar in the two groups. **Closed bars** = AF group; **open bars** = RSR group. *$p < 0.05$, AF vs. RSR. Abbreviations as in Figure 1

The TIMP-1 protein showed a tendency to rise in the AF patients as compared to that in the RSR patients, but it was not significant ($p < 0.1$, Fig. 2A). Interestingly, the expression level of the MMP-9 was also higher in the PAF group than in the RSR group (RSR: PAF, $p < 0.05$, Fig. 2B). The level of the TIMP-1 protein was positively correlated to the left atrial diameter ($p < 0.05$, $R = 0.453$).

The relative expression of the MMP-9 mRNA was higher in the AF group than in the RSR group (Fig. 3A, $p < 0.05$). The difference in the expression of the TIMP-1 mRNA between the two groups was not significant. The ratio of the MMP-9 to TIMP-1 was higher in the AF group than that in the RSR group ($p < 0.05$). Expression of the MCP-1 mRNA was higher in the AF group than in the RSR group, whereas that of the TNF-α mRNA was similar between the groups (Fig. 3B).

Hematoxylin-eosin staining showed that, in the atrium, the cell layer under the epicardium was thicker in the AF group than in the RSR group (Figs. 4A and 4B). In situ zymography revealed that the activity of the gelatinase, represented as unstained spots with Biebrich scarlet in the FIZ-GN films, was higher in patients with AF than in those with RSR (Figs. 4C and 4D). The unstained spots in the FIZ-GN films completely disappeared in the MMP inhibitor-coated FIZ-GI films, meaning that all the spots reflected the activity of the MMP (gelatinase) (Figs. 4E and 4D). The activity of the gelatinase was distributed under the epicardium, in the lumens of blood vessels, and in the interstitium of cardiac myocytes. Gelatinase activity was higher in the AF group than in the RSR group (13.1 ± 2.3% vs. 7.3 ± 2.3%). The left atrial diameter and gelatinase activity were positively correlated (Fig. 5, $p < 0.05$, $R = 0.766$).

Immunohistochemical analysis showed that, in the atria with AF, the MMP-9 was found mainly in the perivascular area, under the epicardium, and sporadically in the interstitium of the cardiomyocytes (Figs. 6A and 6B). Conversely, in the atria with RSR, we could not detect any MMP-9 in the perivascular area, and there were thin layers of the MMP-9 under the epicardium. The staining of the MMP-9 appeared as fibers in the enlarged view (Fig. 6C). In the same place, we observed collagen fibers stained blue with Masson trichrome (Fig. 6D). The double staining of the MMP-9 and CD11b revealed that the distribution of the MMP-9 was not always coincident with that of the CD11b (Fig. 7).

DISCUSSION

Atrial fibrillation is a common arrhythmia (1) and, unfortunately, a potential source of thromboembolic events (2). As AF has a tendency to become persistent due to atrial remodeling, new strategies for early termination of AF should be established by clarifying the mechanisms of the

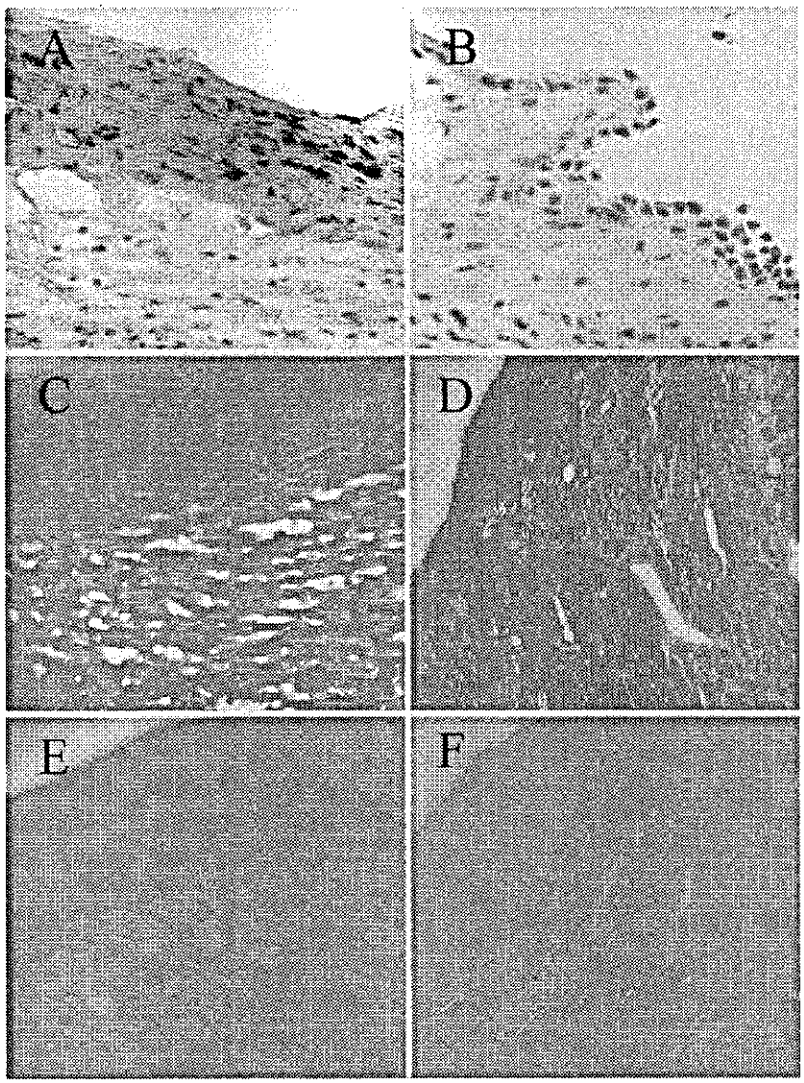

Figure 4. Hematoxylin-eosin staining and in situ zymography in atria with RSR and AF. Hematoxylin-eosin staining showed that the cell layer under the epicardium of the atrium was thicker with AF **(A)** than with RSR **(B)**. In situ zymography showed that the activity of gelatinase, represented as unstained spots from the Biebrich scarlet in the FIZ-GN films, was higher in patients with AF **(C)** than in those with RSR **(D)**. The activity was completely blocked by an MMP inhibitor, which presented as unstained spots in the FIZ-GN films **(E)** and which disappeared in the FIZ-GI films **(F)**. Original magnification: ×200. Abbreviations as in Figure 1.

atrial remodeling induced by AF. Many investigators have demonstrated that changes in the electrophysiological properties occur during AF, and ionic channel remodeling factors, such as a reduction in the L-type Ca^{2+} channels and downregulation of several kinds of potassium channels, have been represented as probable explanations for these changes (10–13). Some researchers have shown that the expression of gap junctions (connexin 40) increased in the atria during AF (15,16). Recently, it was reported that ADAM activity increased in fibrillating human atria (17). These changes in the expression of gap junctions and ADAMs cause structural changes in the atrium that are considered to be part of the pathogenesis of sustained AF. However, there still has been little information about the mechanisms of structural remodeling in the atria with AF.

Matrix metalloproteinases are a family of proteolytic enzymes that regulate the extracellular matrix turnover together with the inhibitory mediators of the MMPs called TIMPs (18,19). The MMPs have been known to be involved in the pathogenesis of many kinds of cardiovascular diseases, including atherosclerosis, restenosis, dilated cardiomyopathy, and MI (20,21). The MMP-1, -2, -3, -9, -13, and -14 exist in the mammalian myocardium. It has also been reported that MMP-9 especially plays a pivotal role in myocardial remodeling in ischemic cardiomyopathy and chronic heart failure (19, 21–25). We selected MMP-1, -2, and -9 to investigate the mechanism of the atrial remodeling by AF in the present study. In addition, compared to the vast information on ventricular myocardial remodeling, there has been little information as to whether or not the MMPs exist in human atrial tissue, and certainly there has been no data on the relationship between the MMPs and the atrial remodeling in AF.

In this study, we first investigated whether or not the

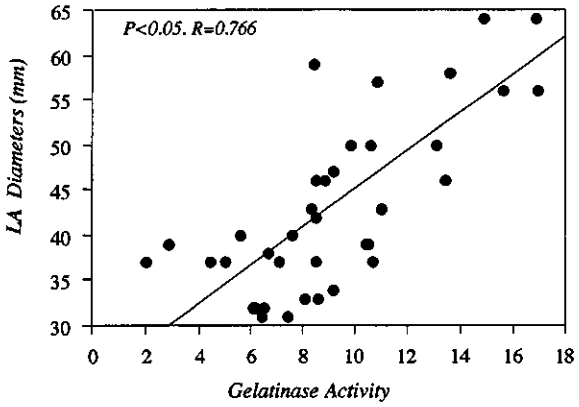

Figure 5. Relationship between the gelatinase activity and left atrial (LA) diameter. The level of gelatinase activity was positively correlated to the left atrial diameter. ($p < 0.05$, $R = 0.766$).

expression of MMP-1, -2, and -9 differed between human atria with AF and with RSR. As a result of Western blotting analysis, the active form of MMP-9 was significantly increased in the AF subjects in comparison to those in the RSR group ($p < 0.05$), but no difference was observed in the protein level of the latent form of the MMP-9 and active and latent forms of the MMP-1 and MMP-2 between the two groups of subjects. Also, the ELISA analysis showed that expression of the MMP-9 in the atria increased step by step, as the rhythm changed from RSR to PAF and from PAF to CAF. As for the TIMP-1, the level of the TIMP-1 protein was positively correlated to the left atrial diameter. The positive correlation between the left atrial diameter and the expression of the TIMP-1 protein suggested that the TIMP-1 protein increased in compensation for the MMP-9 increase. We also demonstrated that the expression of the MMP-9 was more increased in the atria of the AF group than in that of the RSR group, not only for the protein level, but also the mRNA level. Based on these data, the MMP-9 was judged to be a strong candidate for being associated with the atrial structural remodeling during AF. As the MMP-9 overexpressed, the TIMP-1 compensatingly increased, but it did not catch up to the MMP-9 increase, and the balance between them broke down, thus possibly resulting in the atrial structural remodeling of AF.

We first demonstrated the existence and distribution of the MMP-9 in the atrial tissue in the present study. In the atria with AF, the MMP-9 exists mainly in the perivascular area, under the epicardium, and sporadically in the interstitium of cardiomyocytes, whereas in the atria with RSR, it was found only under the epicardium as a thin layer and rarely in the interstitium. The staining of the MMP-9 appeared as fibers, and the image reflected the secreted MMP-9 ridden of collagen fibers.

The MMP-9 is usually found in human and ventricular

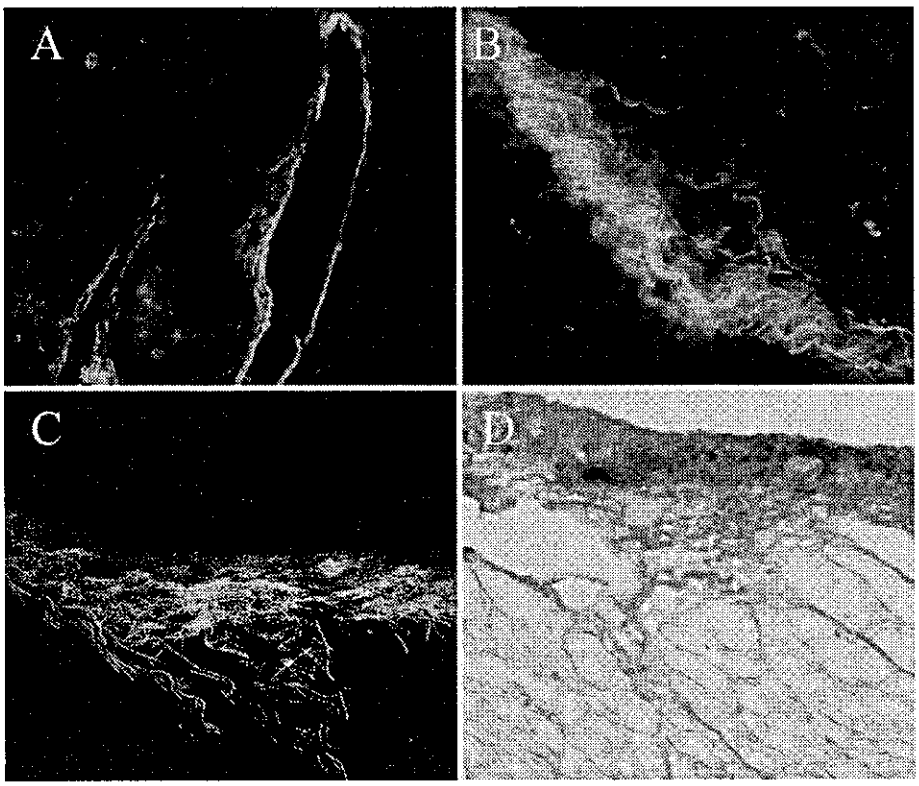

Figure 6. Immunohistochemical analysis of the atria. Immunohistochemical analysis showed that in atria with AF, the MMP-9 exists mainly in the perivascular region **(A)**, under the epicardium **(B)**, and sporadically in the interstitium of cardiomyocites. The staining of the MMP-9 appeared as fibers in the enlarged view **(C)**. In the same region, collagen fibers are stained blue with Masson trichrome **(D)**. Original magnification: **A, B** ×200 and **C, D** ×400. Abbreviations as in Figure 1.

JACC Vol. 43, No. 5, 2004
March 3, 2004:818–25

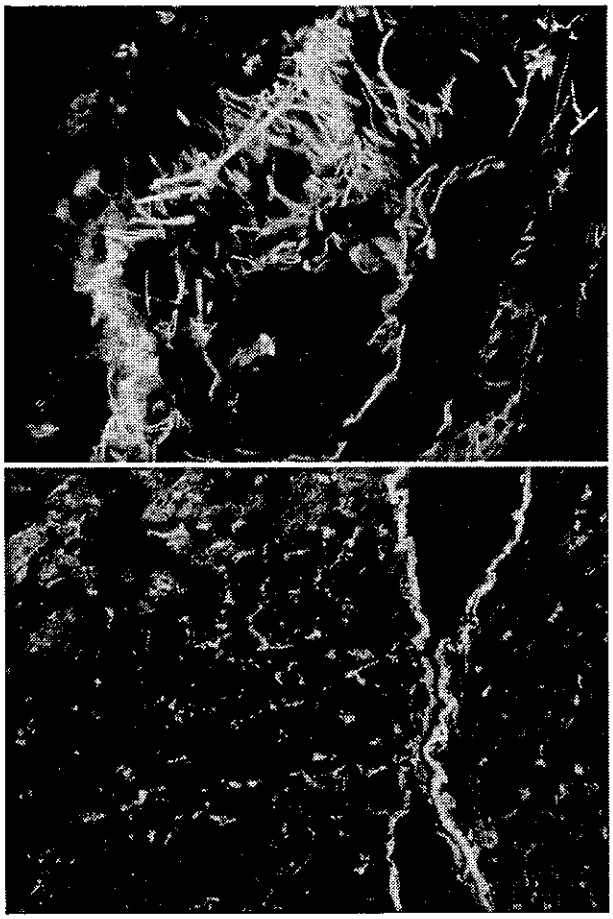

Figure 7. Double staining of the matrix metalloproteinases (MMP)-9 and CD11b in the atria. The double staining of the MMP-9 and CD11b revealed that the distribution of the MMP-9 was not always coincident with that of the CD11b. Original magnification: **upper panel** ×200; **lower panel** ×400.

myocardial remodeling. It has been known to be associated with macrophages, infiltrating neutrophils, fibroblasts, and vascular smooth muscle cells (26–28). Inflammatory changes have been known to contribute to the atrial structural remodeling and to increase the propensity for AF to persist (29). Recently, investigators reported that inflammatory cells indicative of chronic inflammation had infiltrated the dilated atrium (30). Monocyte chemoattractant protein-1 is a type of chemokine, caused by changes in the renin-angiotensin system and shear stress; it is an important mediator in many pathologies recruited by multiple leukocytes, and it is known to be closely related to MMPs (31). In this study, the relative expression of the mRNA of the MCP-1, indicative of chronic inflammation, was higher in the AF group than in the RSR group, but the TNF-α, indicative of acute inflammation, was similar for both groups. However, double staining of the MMP-9 and Mac-1 revealed that the distribution of the MMP-9 did not always coincide with that of the Mac-1, suggesting that the MMP-9 in atria with AF partially originates from blood cells.

Expression of the MMP mRNA can be modulated by various chemical agents, such as neurohormones, corticosteroids, and cytokines influencing the MMP gene expression through the formation of transcription factors binding to specific response elements on the MMP gene promoters (21). The common response elements contained in the promoter region of the MMP genes are known to be activator protein-1 (AP-1) and NF-κB sites (32). The TNF-α, a cytokine, is known to be a contributor to LV myocardial remodeling. Moreover, TNF-α was reported as one of the molecular triggers for the induction of myocardial MMPs in LV remodeling (33). In our study, the relative expression of the TNF-α was similar for both the atria with AF and those with RSR.

In the present study, we clarified that the expression of the MMP-9 had increased in the fibrillating atria, but the mechanism of the MMP-9 increase is the subject of a separate study. The molecular mechanisms of AF were not completely clarified in previous studies, but there was a report that an ACE-dependent increase in the amount of activated extracellular signal-regulated kinases Erk1/Erk2 in atrial interstitial cells might spur on atrial fibrosis in atria with AF (34). Angiotensin II (Ang II) was reported to mediate the upregulation of the matrix gelatinase (MMP-9) and to be related to the cardiac hypertrophy process and cardiac remodeling (35). It was also reported that Ang II blockade prevented myocardial fibrosis, and the long-term combined endothelin-A receptor and ACE inhibition improved cardiac failure (36). Angiotensin II was reported to be involved in the mechanism of the atrial electrical remodeling, and blockade of Ang II may lead to a better therapeutic management of human AF (37). Hence, alterations in the renin-angiotensin system in hearts with AF may be a possible trigger of the MMP secretion.

In conclusion, we clarified that the expression of the MMP-9 increased in the fibrillating atrial tissue, and the alteration in the MMP-9/TIMP-1 may contribute to the atrial structural remodeling and atrial dilation during AF. Additionally, we clarified that the distribution of the MMP-9 was in the perivascular area and under the epicardium in the atria.

Acknowledgments

We especially thank Takafumi Ishida, MD, and Syuichi Nomura, MD, for their excellent advice on this study. We also thank Yoshiko Kondo, Terumasa Hibi (NILS), and Yuka Umeda for their technical assistance, and Yuko Ohmura for her secretarial assistance.

Reprint requests and correspondence: Dr. Yukiko Nakano, Department of Medicine and Molecular Science, Division of Frontier Medical Science, Programs for Biomedical Research, Graduate School of Biomedical Science, Hiroshima University, 1-2-3 Kasumi, Minami-ku, Hiroshima, 734-8551, Japan. E-mail: ynakano@xj8.so-net.ne.jp.

REFERENCES

1. Kannel WB, Abbott RD, Savage DD, et al. Epidemiological features of atrial fibrillation: the Framingham Study. N Engl J Med 1982;306: 1018–22.
2. Murgatroyd FD, Camm AJ. Atrial arrhythmias. Lancet 1993;341: 1317–22.
3. Wijffels MC, Kirchhof CJ, Dorland R, et al. Atrial fibrillation begets atrial fibrillation. A study in awake chronically instrumented goats. Circulation 1995;92:1954–68.
4. Morillo CA, Klein GJ, Jones DL, et al. Chronic rapid atrial pacing. Structural, functional, and electrophysiological characteristics of a new model of sustained atrial fibrillation. Circulation 1995;91:1588–95.
5. Tieleman RG, Van Gelder IC, Crijns HJ, et al. Early recurrences of atrial fibrillation after electrical cardioversion: a result of fibrillation-induced electrical remodeling of the atria? J Am Coll Cardiol 1998; 31:167–73.
6. Goette A, Honeycutt C, Langberg JJ. Electrical remodeling in atrial fibrillation. Time course and mechanisms. Circulation 1996;94:2968–74.
7. Everett TH 4th, Li H, Mangrum JM, et al. Electrical, morphological, and ultrastructural remodeling and reverse remodeling in a canine model of chronic atrial fibrillation. Circulation 2000;102:1454–60.
8. Allessie M, Ausma J, Schotten U. Electrical, contractile and structural remodeling during atrial fibrillation (review). Cardiovasc Res 2002;54: 230–46.
9. Kostin S, Klein G, Szalay Z, et al. Structural correlate of atrial fibrillation in human patients. Cardiovasc Res 2002;54:361–79.
10. Lai LP, Su MJ, Lin JL, et al. Down-regulation of L-type calcium channel and sarcoplasmic reticular $Ca^{(2+)}$-ATPase mRNA in human atrial fibrillation without significant change in the mRNA of ryanodine receptor, calsequestrin and phospholamban: an insight into the mechanism of atrial electrical remodeling. J Am Coll Cardiol 1999;33: 1231–7.
11. Brundel BJ, Van Gelder IC, Henning RH, et al. Ion channel remodeling is related to intraoperative atrial effective refractory periods in patients with paroxysmal and persistent atrial fibrillation. Circulation 2001;103:684–90.
12. Brundel BJ, Henning RH, Kampinga HH, et al. Molecular mechanisms of remodeling in human atrial fibrillation. Cardiovasc Res 2002;54:315–24.
13. Dobrev D, Graf E, Wettwer E, et al. Molecular basis of downregulation of G-protein-coupled inward rectifying K(+) current I(K,ACh) in chronic human atrial fibrillation: decrease in GIRK4 mRNA correlates with reduced I(K,ACh) and muscarinic receptor-mediated shortening of action potentials. Circulation 2001;104:2551–7.
14. Ausma J, Litjens N, Lenders MH, et al. Time course of atrial fibrillation-induced cellular structural remodeling in atria of the goat. J Mol Cell Cardiol 2001;33:2083–94.
15. Polontchouk L, Haefliger JA, Ebelt B, et al. Effects of chronic atrial fibrillation on gap junction distribution in human and rat atria. J Am Coll Cardiol 2002;39:1709–10.
16. van der Velden HM, Ausma J, Rook MB, et al. Gap junctional remodeling in relation to stabilization of atrial fibrillation in the goat. Cardiovasc Res 2000;46:476–86.
17. Arndt M, Lendeckel U, Rocken C, et al. Altered expression of ADAMs (A Disintegrin And Metalloproteinase) in fibrillating human atria. Circulation 2002;105:720–5.
18. Li YY, Feldman AM, Sun Y, McTiernan CF. Differential expression of tissue inhibitors of metalloproteinases in the failing human heart. Circulation 1998;98:1728–34.
19. Thomas CV, Coker ML, Zellner JL, et al. Increased matrix metalloproteinase activity and selective upregulation in LV myocardium from patients with end-stage dilated cardiomyopathy. Circulation 1998;97: 1708–15.
20. Creemers EE, Cleutjens JP, Smits JF, et al. Matrix metalloproteinase inhibition after myocardial infarction: a new approach to prevent heart failure? Circ Res 2001;89:201–10.
21. Spinale FG. Matrix metalloproteinases: regulation and dysregulation in the failing heart. Circ Res 2002;90:520–30.
22. Spinale FG, Coker ML, Heung LJ, et al. A matrix metalloproteinase induction/activation system exists in the human left ventricular myocardium and is upregulated in heart failure. Circulation 2000;102: 1944–9.
23. Ducharme A, Frantz S, Aikawa M, et al. Targeted deletion of matrix metalloproteinase-9 attenuates left ventricular enlargement and collagen accumulation after experimental myocardial infarction. J Clin Invest 2000;106:55–62.
24. Spinale FG, Coker ML, Bond BR, et al. Myocardial matrix degradation and metalloproteinase activation in the failing heart: a potential therapeutic target. Cardiovasc Res 2000;46:225–38.
25. Romanic AM, Harrison SM, Bao W, et al. Myocardial protection from ischemia/reperfusion injury by targeted deletion of matrix metalloproteinase-9. Cardiovasc Res 2002;54:549–58.
26. Henny AM, Wakelet PR, Davies MJ, et al. Localization of stromelysin gene expression in atherosclerotic plaques by in situ hybridization. Proc Natl Acad Sci U S A 1991;88:8154–8.
27. Galis ZS, Sukhova GK, Lark MW, et al. Increased expression of matrix metalloproteinases and matrix degrading activity in vulnerable regions of human atherosclerotic plaques. J Clin Invest 1994;94:2493–503.
28. Bond M, Chase AJ, Baker AH, et al. Inhibition of transcription factor NF-kappa B reduces matrix metalloproteinase-1, 3 and 9 production by vascular smooth muscle cells. Cardiovasc Res 2001;50:556–65.
29. Chung MK, Martin DO, Sprecher D, et al. C-reactive protein elevation in patients with atrial arrhythmia. Circulation 2001;104: 2886–91.
30. Veheule S, Wilson E, Everett T, et al. Alterations in atrial electrophysiology and tissue structure in a canine model of chronic atrial silatation due to mitral regurgitation. Circulation 2003;107:2615–22.
31. McQuibban GA, Gong JH, Wong JP, et al. Matrix metalloproteinase processing of monocyte chemoattractant proteins generates CC chemokine receptor antagonists with anti-inflammatory properties in vivo. Blood 2002;100:1160–7.
32. Bond M, Fabunmi RP, Barker AH, et al. Synergistic upregulation of metalloproteinase-9 by growth factors and inflammatory cytokines: an absolute requirement for transcription factor NF-κB. FEBS Lett 1998;435:29–34.
33. Bradham WS, Bozkurt B, Gunasinghe H, et al. Tumor necrosis factor-alpha and myocardial remodeling in progression of heart failure: a current perspective. Cardiovasc Res 2002;53:822–30.
34. Goette A, Staack T, Rocken C, et al. Increased expression of extracellular signal-regulated kinase and angiotensin-converting enzyme in human atria during atrial fibrillation. J Am Coll Cardiol 2000;35:1669–77.
35. Rouet-Benzineb P, Gontero B, Dreyfus P, et al. Angiotensin II induces nuclear factor–kappa-B activation in cultured neonatal rat cardiomyocytes through protein kinase C signaling pathway. J Mol Cell Cardiol 2000;32:1767–78.
36. Fraccarollo D, Bauersachs J, Kellner M, et al. Cardioprotection by long-term ET(A) receptor blockade and ACE inhibition in rats with congestive heart failure: mono- versus combination therapy. Cardiovasc Res 2002;54:85–94.
37. Nakashima H, Kumagai K, Urata H, et al. Angiotensin II antagonist prevents electrical remodeling in atrial fibrillation. Circulation 2000; 101:2612–7.

Archives of Oral Biology (2004) 49, 739–746

Available online at www.sciencedirect.com

SCIENCE DIRECT®

Archives of Oral Biology

www.intl.elsevierhealth.com/journals/arob

Immuno-localization of COX-1 and COX-2 in the rat molar periodontal tissue after topical application of lipopolysaccharide

M. Miyauchi[a], M. Hiraoka[a], H. Oka[a], S. Sato[a], Y. Kudo[a], I. Ogawa[b], K. Noguchi[c], I. Ishikawa[c], T. Takata[a,*]

[a]*Division of Frontier Biomedical Science, Department of Oral Maxillofacial Pathobiology, Graduate School of Biomedical Sciences, Hiroshima University, Hiroshima 734-8553, Japan*
[b]*Center of Oral Clinical Examination, Hiroshima University Hospital, 1-2-3, Kasumi, Minami-ku, Hiroshima 734-8553, Japan*
[c]*Division of Periodontology, Department of Hard Tissue Engineering, Graduate School, Tokyo Medical and Dental University, 1-5-45, Yushima, Bunkyo-ku, Tokyo 113-8549, Japan*

Accepted 6 April 2004

KEYWORDS
Cyclooxygenase-2;
Lipopolysaccharide;
Immunohistochemistry;
Periodontitis;
Rat model

Summary Up-regulation of prostaglandin E_2 (PGE_2) production in the periodontal tissue is considered to be important for periodontal tissue destruction. The purpose of the study was to demonstrate the dynamic changes of immuno-localization of cyclooxygenase-1 (COX-1) and cyclooxygenase-2 (COX-2) in rat periodontal tissue after topical application of lipopolysaccharide (LPS: 5 mg/ml in physiological saline) from *Escherichia coli* into the rat molar gingival sulcus. In the normal periodontal tissue, small numbers of junctional epithelium (JE) cells and numerous osteocytes embedded in alveolar bone constitutively expressed COX-1. The COX-1 expression was not effected by LPS application. JE cells, especially in the coronal portion of JE also expressed COX-2. LPS application induced the JE cells with consequent transient expression of COX-2 with a peak at day 1. These findings suggest that JE cells may play a critical role in first defense line against LPS challenge and PGE_2 from JE cells may be responsible for the initiation of periodontal inflammation. In the deep periodontal tissue, cementoblasts and osteoblasts showed constitutive expression of COX-2, which may be induced by continuous cyclic tension force due to occlusal pressure. LPS application caused a transient up-regulation of COX-2 expression in periodontal ligament fibroblasts, cementoblasts and osteoblasts. It is suggested that the inducible production of PGE_2 via COX-2 by these cells may be associated with connective tissue destruction and alveolar bone resorption.

Superficial periodontal tissues are constantly exposed to plaque-associated bacteria and bacterial lipopolysaccharide (LPS), which can induce inflammatory reaction and consequent tissue destruction. LPS induces a variety of products from various host cells such as interleukin-1 (IL-1, tumor necrosis factor (TNF) and prostaglandins (PGs).[1,2] In particular, PGs are well known as potent soluble mediators in normal biological functions[3] and in various inflammatory lesions.[4–6]

*Corresponding author. Tel.: +81-82-257-5631; fax: +81-82-257-5619.
E-mail address: ttakata@hiroshima-u.ac.jp (T. Takata).

0003-9969/$ – see front matter © 2004 Elsevier Ltd. All rights reserved.
doi:10.1016/j.archoralbio.2004.04.004

The cyclooxygenase (COX) is the first and critical enzyme involved in the metabolism of arachidonic acid. COX acts on arachidonic acid to form PGG_2 and reduces PGG_2 to PGH_2, which is the immediate precursor of PGs, by its peroxidase activity.[7] Recently two isoforms of COX have been characterized and named COX-1 and COX-2. COX-1 is responsible for constitutive PGs production under physiological condition in various tissues such as kidney and stomach,[3] PGs produced by COX-1 are tissue protective and maintain normal function. On the other hand, COX-2 expression is inducible by cytokines, growth factors and LPS and a large amount of PGs is produced by COX-2 in inflammatory lesions.[8,9] The two isoforms are encoded by different genes.[10,11]

It has been reported that PGE_2 may mediate pathological bone resorption in periodontitis[12,13] and is associated with attachment loss.[14–16] Furthermore, non-steroidal anti-inflammatory drugs (NSAIDs) were shown to reduce alveolar bone loss associated with periodontal disease[17]. Several studies have demonstrated that PGs produced by inducible COX-2 are involved in the pathogenesis of periodontitis.[18–20] However, the localization of the COX-1 and COX-2 in in vivo periodontal tissues during development of periodontal disease has not been determined.

In previous studies, we have used an experimental model in which initial periodontal tissue destruction is provoked by the topical application of 5 mg/ml LPS from *Escherichia coli (E. coli)* into the rat gingival sulcus. Infiltration of polymorphonuclear leukocytes and macrophages, vascular dilatation and inflammatory edema in the subepithelial gingival connective tissue,[21,22] enhancement of collagen phagocytosis by periodontal ligament fibroblasts[23] and stimulation of osteoclastic bone resorption[21] were observed in this animal model. Furthermore, we demonstrated transient production of proinflammatory cytokines and suggested that proinflammatory cytokines released from host cells may cause various histological changes in the periodontal tissue.[24] Considering the induction of COX-2 by proinflammatory cytokines, the subsequent production of PGs via inductive COX-2 and a role of PGs as a potent mediator of periodontal tissue destruction, we hypothesized that COX-2 may be activated in periodontal tissue during an acute inflammatory episodes in this animal model.

The aim of this study was to demonstrate the dynamic changes in the immuno-expression of COX-1 and COX-2 in rat periodontal tissues after topical application of LPS in the gingival sulcus. The roles of the COX-1 and COX-2 in periodontal tissue destruction were discussed.

Materials and methods

Animal experiment

A total of thirty-five, 7 week-old (about 190 g), male Wistar Strain rats were used in this study. They were divided into seven groups of five rats each. Under the intraperitoneal anesthesia of 20% ethyl carbamate (100 mg/100 g body weight), a rat was fixed on his back on an experimental stand. A cotton roll (2 mm in diameter and 1 cm in length) saturated with 5 mg/ml LPS from *E. coli* (Sigma Chemical Co., St. Louis, MO U.S.A.) in sterile physiological saline (Otsuka Med. Co., Tokyo Japan) was placed on the occlusal surface of the right and left upper molar regions for 1 h. The cotton roll was changed every 20 min. Three rats each were killed at 1, 3 h or 1, 2, 3 or 7 days after the LPS treatment by an overdose of ethyl ether. The remaining 5 rats were used as an untreated control group.

The experimental protocol was approved by the animal care committee of Hiroshima University.

Tissue preparation

Tissue samples were resected en bloc from the right and left upper molar regions and fixed for 8 h in a periodic-lysin paraformaldehyde solution at 4 °C. The samples were cut into two parts, which included the first or second molar (about 2 mm thick), respectively at the buccopalatal plane parallel to each disto-palatal root. They were then decalcified in a 10% ethylenediaminetetraacetate (EDTA) solution in a phosphate buffered saline (PBS) (pH. 7.4) for 5 days at 4 °C. The decalcified tissue blocks were embedded in OCT compound (Tissue Tec, Miles Scientific, Naperville, IL). Serial frozen sections (8 μm thick) parallel to the long axis of the tooth, including the root apex were cut and collected on glass slides.

Immunohistochemistry

The following immunostaining was carried out using a DAKO-LSB2 kit (DAKO Co., Carpinteria, CA). After washing in PBS, each section was incubated with 0.25% casein in PBS for 30 min at 4 °C and then incubated with antibodies to COX-1 and COX-2 chemokines for 24 h at 4 °C in humid atmosphere. The COX-1 monoclonal antibody and COX-2 polyclonal antibody (Cayman Chemical, Ann Arbor, MI) were diluted in 0.001 M PBS containing 5% normal rat serum to 1/200 and 1/500, respectively. After being rinsed with PBS the sections were incubated with biotinylated secondary antibody for 30 min. The sections were rinsed in PBS and immersed in

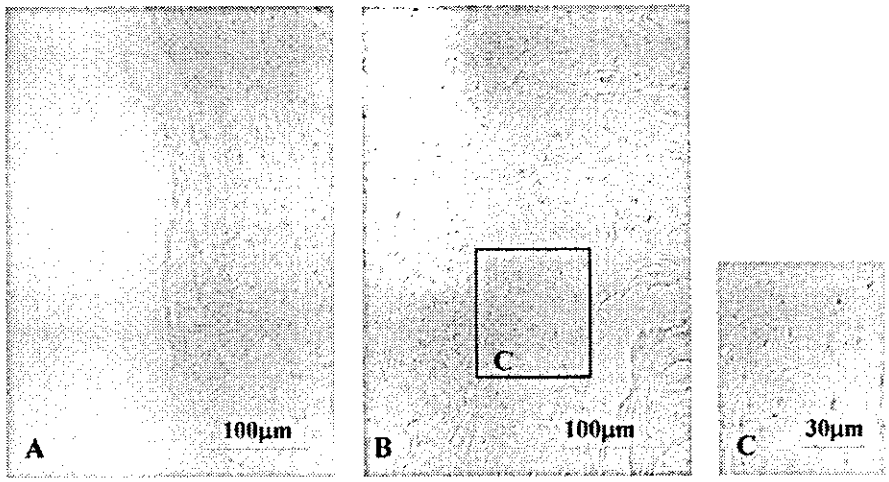

Figure 1 Immunohistochemical staining of COX-1 in the periodontal tissue of an untreated control rat. (A) Weakly positive staining is seen in the junctional epithelial cells facing the enamel surface. (B) Osteocytes embedded in alveolar bone stained weakly positive for COX-1. (C) Note positively stained osteocytes.

0.3% hydrogen peroxide in PBS to block the endogenous peroxidase activity for 1 h. The sections were rinsed with PBS, incubated with the peroxidase-conjugated streptavidin for 30 min and rinsed with PBS again. The color was developed with 0.025% 3-3′-diaminobenzidine tetrahydrochloride in Tris-HCl buffer plus hydrogen peroxide (Kyowa medics, Tokyo, Japan). The specimens were counter stained with Mayer's hematoxylin, dehydrated and then mounted.

Specificity was ascertained by substituting PBS and normal rabbit serum for each antibody.

Results

Untreated control periodontal tissue

In the normal gingival tissue of untreated control rats, small number of PMNs was seen in the junctional epithelium (JE) and sub-JE area but no obvious inflammatory changes were observed.

COX-1-positive cells were detected in the layer of JE, which faced the enamel surface (Fig. 1A). In the deep periodontal tissue, numerous osteocytes embedded in alveolar bone were weakly positive

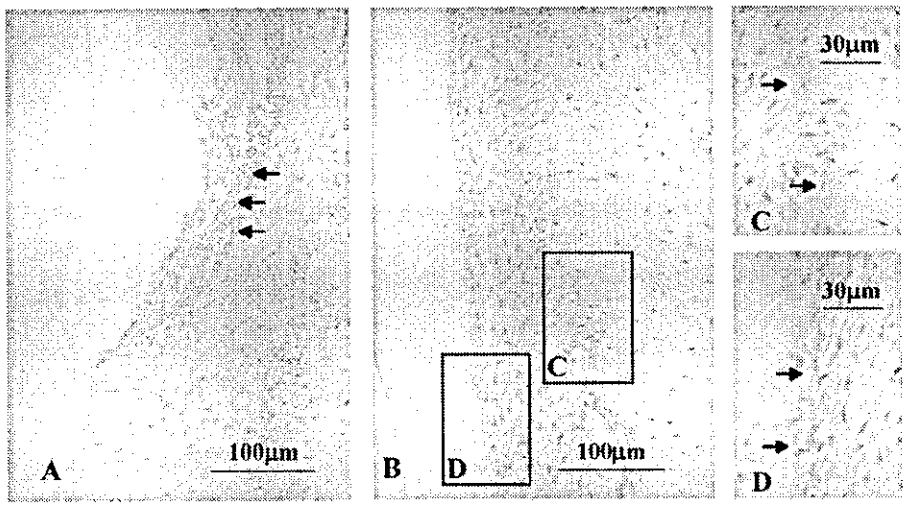

Figure 2 Immunohistochemical staining of COX-2 in the periodontal tissue of an untreated control rat. (A) Positive reaction is seen in the junctional epithelial cells located in the interfacing area to the oral sulcular epithelium (arrows) and macrophages in perivascular area. (B) Note osteoblasts and cementoblasts in the square area. (C) Arrows show positively stained osteoblasts lining the alveolar bone margin (periodontal ligament side). (D) Cementoblasts (arrows) are slightly positive for COX-2.

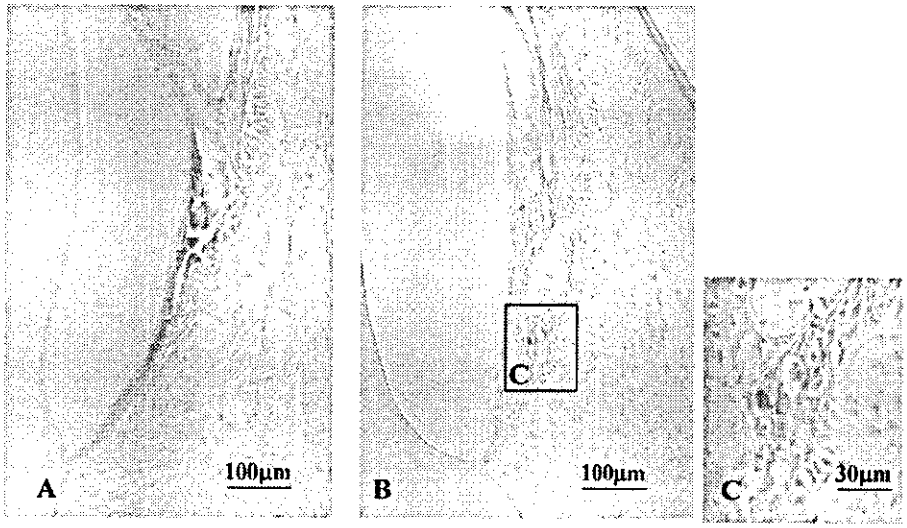

Figure 3 Immunohistochemical staining of COX-2 in the gingival tissue of LPS treated experimental rat. (A) At 1 h after topical application of LPS, almost all cells in the junctional epithelium are strongly positive for COX-2. (B, C) At 2 days after topical application of LPS, numerous COX-2 positive PMNs were seen in the enlarged spaces between COX-2 positive junctional epithelial cells and subjunctional epithelial area.

for COX-1 (Fig. 1B and C). Positive reaction for COX-1 could not be detect in other constitutive cells presented in periodontal tissue. A weakly positive reaction for COX-2 was seen not only in a small number of JE cells adjacent to the gingival sulcus but also in macrophages located in perivascular area (Fig. 2A). Osteoblasts lining the alveolar margin (Fig. 2B and C) and cementoblasts facing the cementum surface (Fig. 2B and D) were also weakly positive for COX-2.

LPS applied periodontal tissue

LPS application caused edematous changes, dilatation of blood capillaries and infiltration of PMNs in sub-JE area. Numerous PMNs migrated into enlarged intercellular spaces of the JE. These findings have appeared in 1-h specimens and continued until 3 days after LPS application. The inflammatory changes gradually decreased with time and disappeared by day 7.

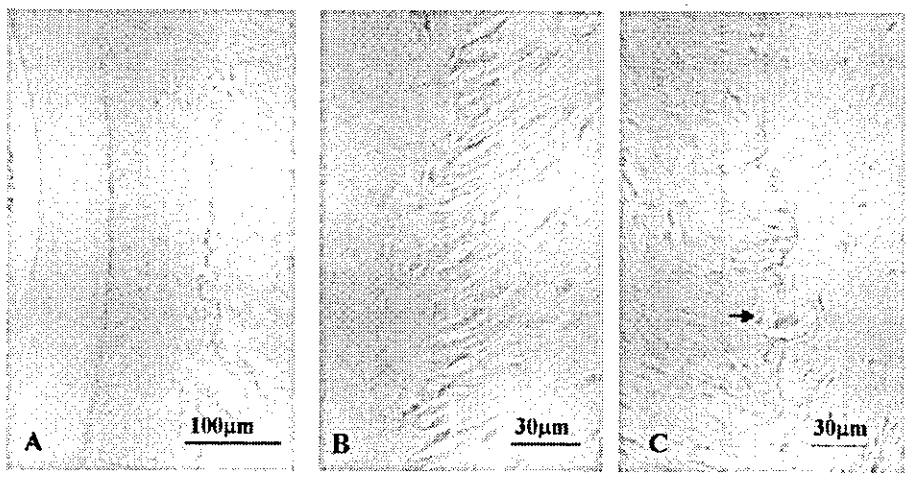

Figure 4 Immunohistochemical staining of COX-2 in the periodontal tissue of LPS treated experimental rat at 2 d after topical application of LPS. (A) Almost all cells facing the root surface and alveolar bone margin (periodontal ligament side) are strongly positive for COX-2. (B) Note the restriction of the cytoplasmic reaction to the tooth surface portion of cementoblasts. (C) The cytoplasmic reaction in osteoblasts is restricted to the alveolar bone side. An osteoclast (arrow) near the COX-2-positive osteoblasts is negatively stained.

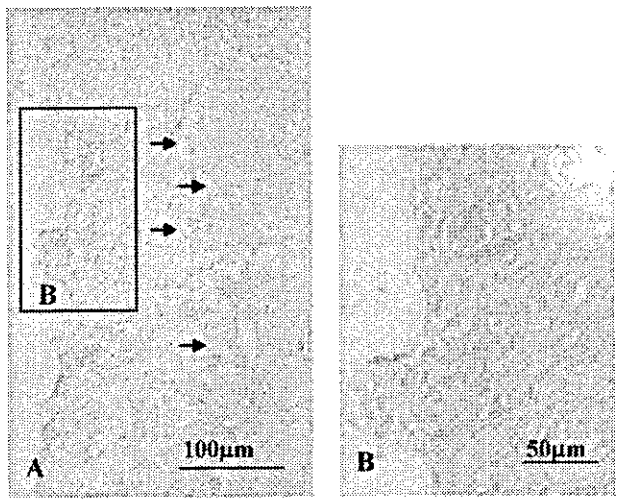

Figure 5 Immunohistochemical staining of COX-2 in the case with prominent periodontal tissue destruction of an LPS treated experimental rat at 3 d after topical application of LPS. (A) Strongly COX-2-expressed cells are seen in the alveolar crestal area of the periodontal ligament. Numerous osteoclasts (arrows) appearing along the alveolar bone margin were negative for COX-2. (B) The COX-2-expressed cells are round and spindle in shape.

LPS enhanced COX-2 expression in periodontal tissue at 3 h. In JE, numerous COX-2-positive cells were observed. Both of the number of COX-2-positive cells and the intensity of COX-2 expression reached a maximum at 1 day (Fig. 3A) and continued for 2 days (Fig. 3B). COX-2-positive epithelial cells were not detected in oral sulcular and oral gingival epithelium. Numerous PMNs with weak positivity for COX-2 were seen in the widely enlarged intercellular spaces among the COX-2 positive JE cells.

In deep periodontal tissue, an enhancement of COX-2 expression in osteoblasts and cementoblasts was detected (Fig. 4A). Almost all cells facing the root surface and alveolar bone surface, which seemed to be cementoblasts (Fig. 4B) and osteoblasts (Fig. 4C) respectively, were positively stained for COX-2 until 2 days after LPS application. Positive reaction in both of cementoblasts and osteoblasts was restricted to the cytoplasm facing to the tooth surface and the bone surface. In the case with severe periodontal tissue destruction at 3 days after, some COX-2-positive periodontal ligament cells, which were spindle or oval in shape, were seen near the resorbing bone and tooth surfaces (Fig. 5A and B). Osteoclasts increased in this period were negatively stained for COX-2 (Figs. 4C and 5A). The intensity of COX-2 expression and the number of COX-2 positive cells decreased and returned to the normal range by 7 days.

On the other hand, the density and distribution pattern of COX-1-positive cells in gingival and periodontal tissue remained unchanged during the experimental period.

Discussion

Since we employed a cotton roll applicator saturated with the LPS solution to avoid the periodontal tissue destruction caused by the application method, we needed a large amount of LPS to perform the present animal experiment. Therefore we used commercially available LPS from *E. coli* to provoke the initial periodontal tissue destruction in this study. *E. coli* is not a periodontal pathogen, but it is evident that LPS from *Actinobacillus actinomycetemcomitans*, which is one of principal periodontal pathogens, is similar to *E. coli*-LPS and shares numerous biological activities on the host cells with *E. coli*-LPS.[25]

We could successfully demonstrate the immunohistochemical localization of COX-1 and COX-2 in rat periodontal tissues. In the untreated control group, the weakly positive COX-1 reaction was observed in JE cells and osteocytes of alveolar bone. The density and distribution pattern of COX-1-positive cells in periodontal tissues remained unchanged during the experimental period. Several studies have reported that COX-1 is widely distributed and constitutively expressed in various cells, where PGs are needed for normal physiological function.[3] For example, the integrity of the stomach lining and normal renal function in the kidney are maintained by PGs synthesized by COX-1. It has been reported that the COX-1 protein expression in human OGE cells was not effected by stimuli of proinflammatory cytokine or serum.[26] In osteocyte-like MLO-Y4 cells, COX-1 mRNA is constitutively expressed and its level remained constant after mechanical strain.[27] The constitutive PGs production, which depends on COX-1, may play an important role on regulation of physiological functions in JE and alveolar bone.

In the untreated control group, not only COX-1 expression but also COX-2 expression was detected. COX-2 is weakly expressed in JE cells osteoblasts and cementoblasts. We previously observed that the coronal half of JE was positively stained for proinflammatory cytokines such as TNF-α, IL-1α and IL-1β in the normal gingival tissue.[24] It has been reported that keratinocytes can constitutively produce proinflammatory cytokines in vitro.[28] The cytokines have been demonstrated to be potent stimulator of PGE_2 production in a variety of cells.[29] These proinflammatory cyto-